CHAPTER 4: RESULTS AND DISCUSSION

In this chapter, results and discussions of numerous experiments carried out throughout the investigation are included. The outcomes of ECR of nitrate using spatially suspended Ag-PVA beads in an undivided cell, as well as divided cell, and the effects of various operational parameters including catalyst concentration, cathode material, current density, initial nitrate concentration, and reusability of Ag-PVA beads studied in the divided cell, are discussed in Section 4.1. The results of ECR of nitrate using spatially suspended AgMPs in undivided and divided cells and the effects of various operational parameters including catalyst concentration, inter-electrode distance, cathode material, initial nitrate concentration, oxidation of ammonia at anode in divided cell and reusability of AgMPs in divided cell are shown in Section 4.2. The involvement of catalysts (Ag-PVA beads and AgMPs) in the production of intermediates and the mechanism of ECR of nitrate are covered in Section 4.3. The outcomes of ECR of nitrate in real water (groundwater) are described in Section 4.4. The removal of high nitrate concentration from simulated metal finishing wastewater using Ti/Co_3O_4 electrode by ECR process and the effects of different parameters including initial nitrate concentration, current density, and reusability of Ti/Co_3O_4 are described in section 4.5. Additionally, section 4.5 includes results of struvite formation and the effect of the molar ratio of Mg:NH_4:PO_4 on struvite formation. Lastly, 4.6 includes references used in this chapter.

4.1 ECR of Nitrate using Ag-PVA beads as a spatially suspended catalyst

The morphological study of Ag-PVA beads was carried out using SEM and EDAX. Experiments were conducted in undivided as well as divided cells. This section represents the results of nitrate reduction in undivided cell and divided cell and the effects of various parameters in divided cell.

4.1.1 Morphological study of Ag-PVA beads

The SEM analysis of a cross-section of an Ag-PVA bead is shown in Figure 9. It may be seen from Figure 9 that most of the silver metal particles were deposited on the bead's surface, which is discernible as a dazzling outer layer. Additionally, the silver layer's thickness is constant across the whole surface indicating uniform deposition. The

related EDAX analyses of a whole bead and a close-up of its periphery are shown in Figure 10 (a) and (b), respectively. The silver content of the bead is extremely low throughout (Figure 10a), and it virtually doubles in the close-up view of the peripheral portion. This shows that the majority of the silver metal particles are immobilised on the sphere's surface and are therefore easily accessible for the catalytic process.

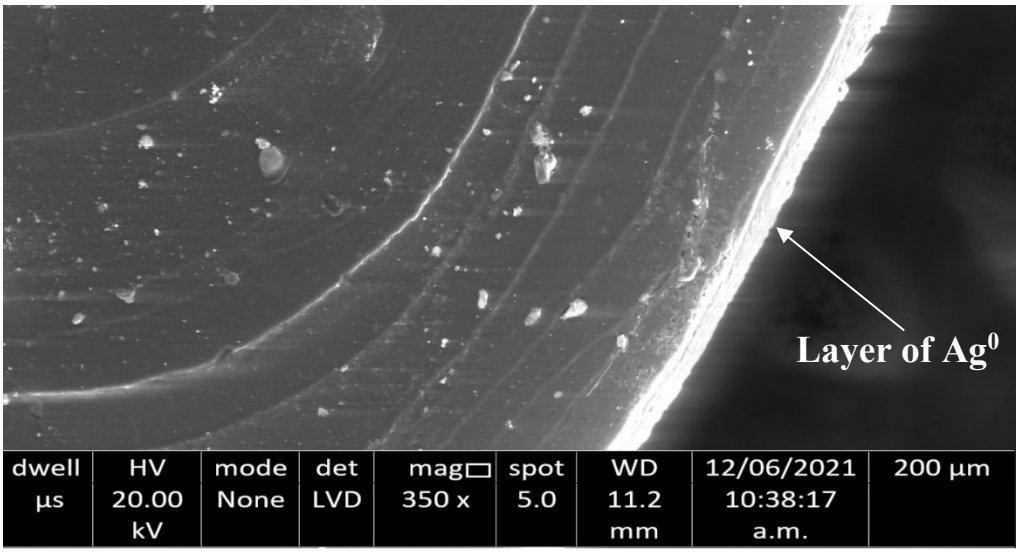

Figure 1 : SEM analysis of Ag-coated PVA bead

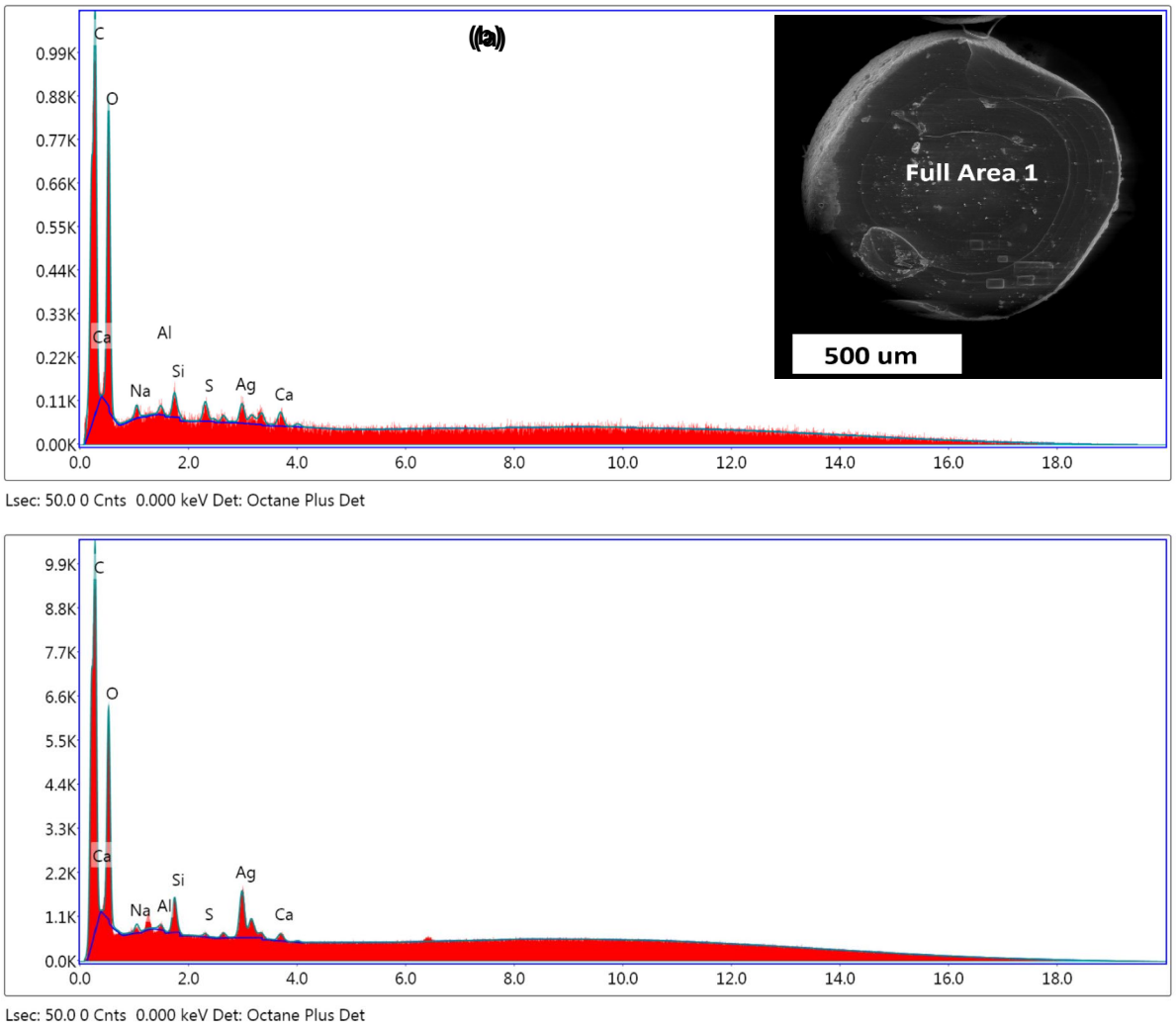

Figure 2 : EDAX spectra of Ag-PVA bead (a), and Ag coated on the surface of PVA bead (b). The inset pictures show the respective SEM images.

4.1.2 Nitrate removal in an undivided cell

Figure 11 shows NO_3-N reduction in an undivided cell with Fe as the cathode and Gr as the anode at a current density of 15 mA/cm^2 in both the absence and presence of 6.67mM Ag-PVA beads as catalyst. There was no evidence of TN elimination in the undivided cell since the nitrate reduction was just 13%, with the end-products being 8% NH_3-N and 5% NO_2-N. Yet, in the presence of Ag-PVA beads, 28% of the original nitrate was eliminated, producing NH_3-N as the final by-product. It was significant to notice that the brown colour of the Ag-PVA beads diminished when introduced to an undivided cell, most likely as a result of the oxidation of the Ag metallic particles on the beads. Thus, the removal of nitrate in an undivided cell was low irrespective of the presence or the absence of Ag-PVA beads.

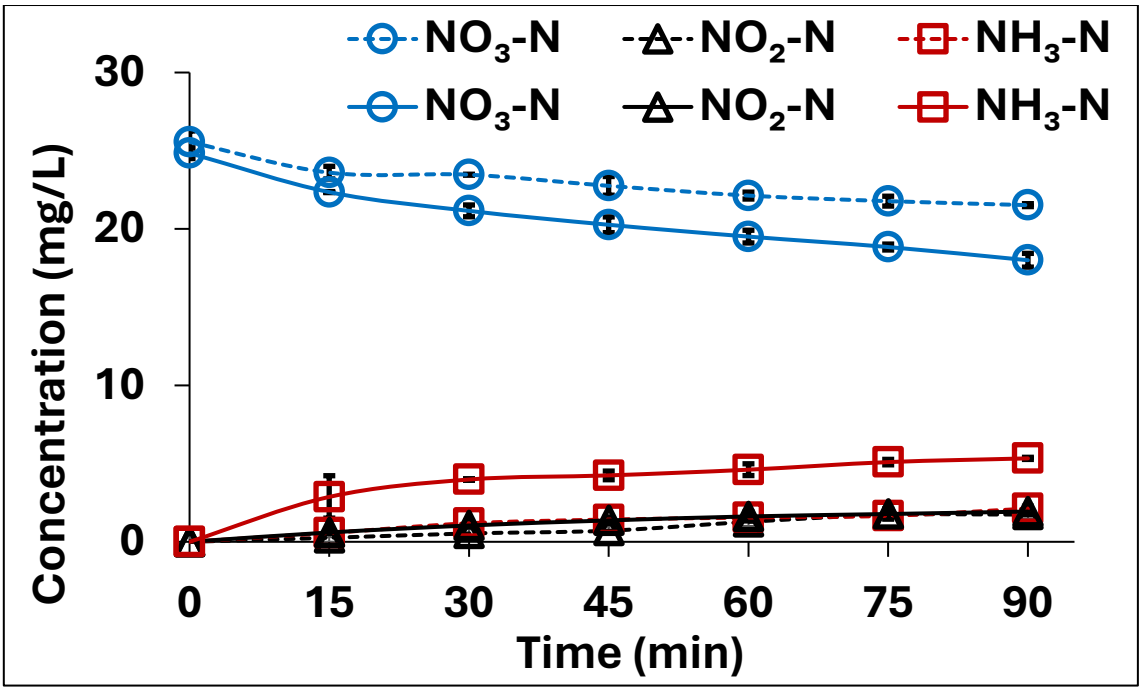

Figure 3 : Undivided cell - Time course profile of NO_3-N removal in the absence (dotted line) and presence (solid line) of Ag-PVA beads

(Reaction conditions: cathode: Fe, anode: Gr, NO_3-N: 25mg/L, Na_2SO_4 as electrolyte: 2g/L, Ag-PVA beads: 6.67 mM, current density: 15mA/cm^2, reaction time: 90min)

The published research reports that nitrate removal in undivided cells is much lower than that in divided cells. For instance, Dash & Chaudhari (2005) reported that after a 9-hour reaction at 140 mA/cm^2 current density, the reduction of nitrate in an undivided cell utilising Gr electrode was restricted to 8%. According to Ding et al. (2015), the removal of nitrate from an undivided cell was about 7 times lower than that of a divided cell. Further research was carried out utilising a divided cell due to the ineffectiveness of nitrate reduction in an undivided cell.

4.1.3 Nitrate removal in a divided cell

The results of nitrate reduction utilising Fe cathode and Gr anode in a divided cell in the absence and presence of 6.67mM Ag-PVA beads as catalyst are shown in Figure 12. Both in the absence and presence of Ag-PVA beads, the nitrate elimination followed the 1st-order reaction kinetics. It should be emphasised that the nitrate reduction rose to 85% in the presence of 6.67mM Ag-PVA beads as opposed to 70% in the absence of beads.

Although this improvement in removal was little, it is crucial to remember that the TN removal climbed to 52% as opposed to 16% in the absence of beads. Hence, the addition of beads boosted the selectivity towards nitrogen synthesis as well as enhanced the nitrate reduction.

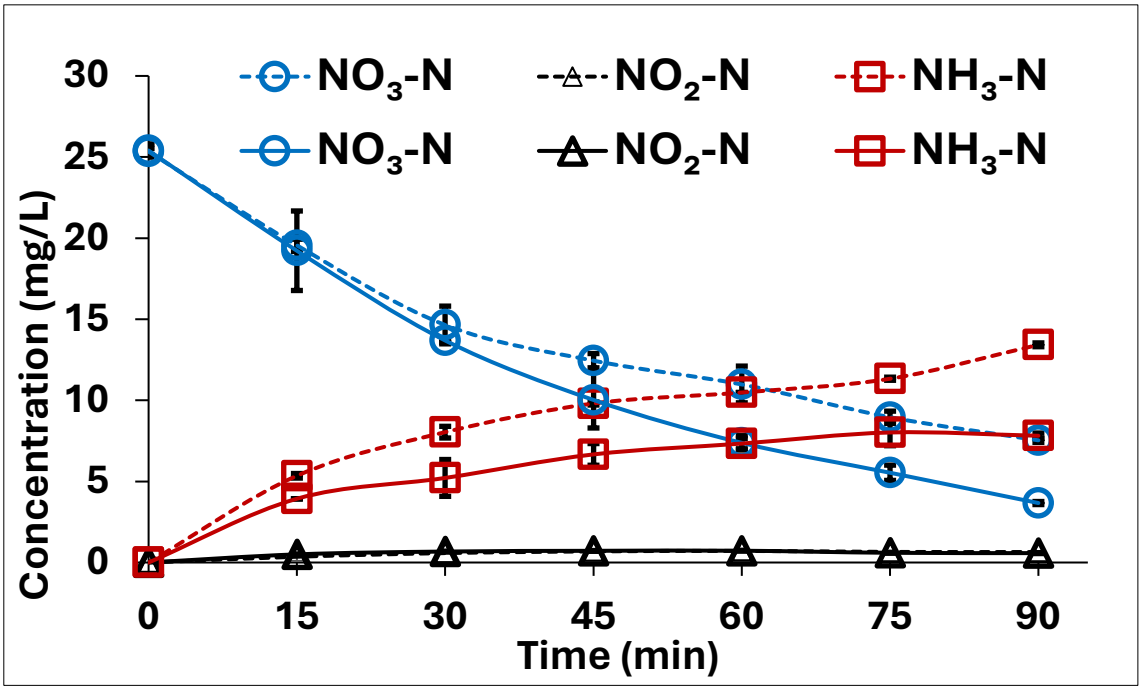

Figure 4 : Divided cell - Time course profile of NO_3-N removal in the absence (dotted line) and presence (solid line) of Ag-PVA beads

(Reaction conditions: cathode: Fe, anode: Gr, NO_3-N: 25mg/L, Na_2SO_4 as electrolyte: 2g/L, Ag-PVA beads: 6.67 mM, current density: 15mA/cm^2, reaction time: 90min)

According to Zhang et al. (2016) , in a divided cell ammonia was the main product of nitrate reduction in the absence of a catalyst however, the inclusion of a Pd-Cu/-alumina catalyst changed the selectivity towards N_2. Due to greater nitrate removal and greater selectivity toward the formation of nitrogen, further studies were conducted in the divided cell in the presence of Ag-PVA beads.

Lei et al. (2022) investigated electro reduction of nitrate using silver surface. Authors coated Ag on a ZnO (zinc oxide) nano wall, and they achieved 66% of nitrate reduction at -0.6V applied potential. The distinct surface-enhanced Raman signals (SERS) of N=O, HNH, and NH_3 showed that nitrite, ammonia, and nitrogen were produced at the end.

4.1.3.1 Effect of concentration of Ag-PVA beads

Table 3 displays the impact of different catalyst concentrations on the nitrate reduction, the mass activity of the catalyst (mg NO_3-N removed per g Ag per min), and selectivity towards NO_2-N ($S_{NO_2\text{-}N}$), NH_3-N ($S_{NH_3\text{-}N}$), and N_2-N ($S_{N_2\text{-}N}$) in a divided cell. The catalyst concentrations are 5, 6.67, and 8.33 mM (≈ 730 Ag-PVA beads). Figure 13 describes nitrate removal and end-products generated at 15mA/cm^2 current density for 90min reaction time using Fe as cathode and Gr as anode. It may be noted that that using 5 and 8.33mM Ag-PVA beads, the nitrate reduction was 77 and 70%, respectively, while using 6.67mM Ag-PVA beads, the maximum reduction of 85% was attained. It is noteworthy to observe that the selectivity of the final products was also impacted by the catalyst concentration. The selectivity for N_2-N production was lowest (19.4%) and greatest (78%) in the presence of 5 and 6.67 mM Ag-PVA, respectively. While the mass activity was lower at 6.67 mM Ag-PVA than at 5 mM, the selectivity for the production of N_2-N was highest and that for NH_3-N was lowest (62.1 and 37.7%, respectively). As a result, 6.67mM Ag-PVA beads were chosen as the ideal dosage for further research.

Beltrame et al. (2020) investigated electrochemical nitrate removal using Pd-coated alumina pellets as a catalyst with various Pd contents (1%wt. Pd, 2.5%wt. Pd, and 5%wt. Pd loaded pellets). According to the authors, nitrate removal dropped from 59% at 1% wt Pd loading to 50% at 5% wt Pd content.

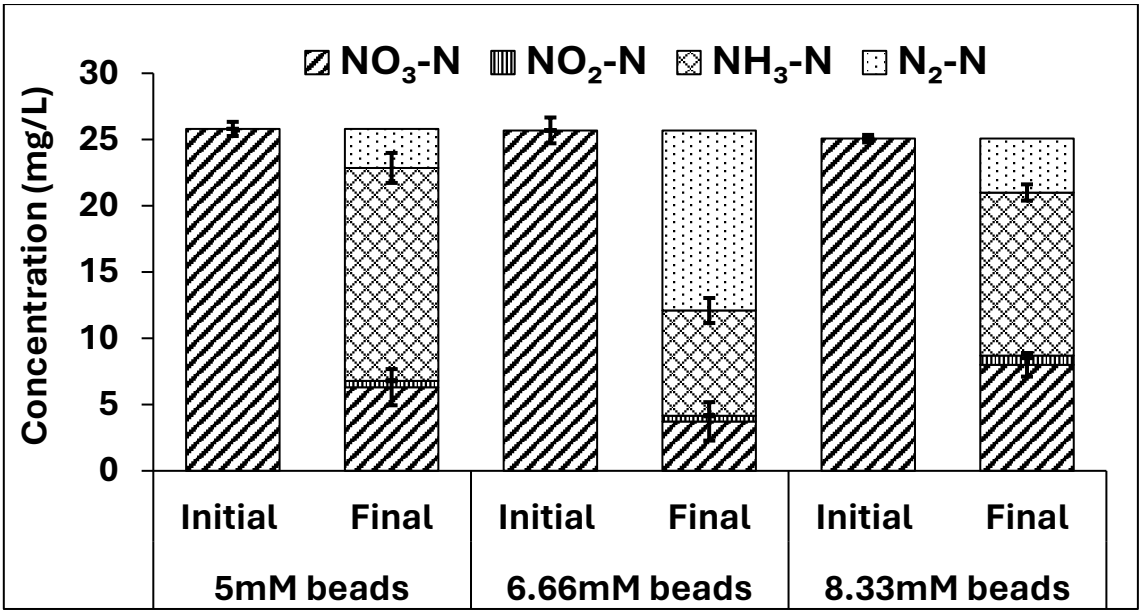

Figure 5 : Removal of NO_3-N with various catalyst concentrations

(Reaction conditions: cathode: Fe, anode: Gr, NO_3-N: 25mg/L, Na_2SO_4 as an electrolyte: 2g/L, current density: 15mA/cm^2, reaction time: 90min)

Table 1: Effect of Ag-PVA catalyst dose on nitrate reduction and selectivity for end-products

Catalyst Dose	Nitrate conversion (%)	Mass Activity (mg of NO_3-N removed/min/gm of Ag)	Concentration of NO_2-N (mg/L)	Concentration of NH_3-N (mg/L)	$S_{NO_2\text{-}N}$ (%)	$S_{NH_3\text{-}N}$ (%)	$S_{N_2\text{-}N}$ (%)
5mM	77±0.9	0.40	0.48	16.05	2.6±0.7	78.0±1.6	19.4±0.7
6.67mM	85±0.5	0.36	0.43	7.93	1.2±0.9	37.7±1.0	62.1±0.8
8.33mM	70±1.2	0.22	0.69	2.9	2.9±1.6	64.3±0.4	32.9±0.6

Reaction conditions: NO_3-N: 25mg/L, cathode: Fe, anode: Gr, Na_2SO_4: 2g/L as electrolyte, current density: 15mA/cm^2, reaction time: 90 min

* Note: To calculate the selectivity for end-products, nitrate removal (%) is considered to be 100%.

4.1.3.2 Effect of cathode material

For nitrate removal, a variety of materials including SS, Fe, Fe/Sn, Cu, and Ti were employed as cathodes. To examine the simultaneous impact of Ag-PVA beads and the cathode material, experiments were conducted both in the absence and presence of a catalyst. Table 4 shows the details of nitrate conversion with different cathode materials in the absence and presence of 6.67mM Ag-PVA beads, as well as the selectivity for ammonia (S_{NH_3-N}), nitrite (S_{NO_2-N}), and nitrogen (S_{N_2-N}). The cathode material and the presence of Ag-PVA beads have an impact on nitrate removal and selectivity of end-products, as shown in Table 4. Overall, it should be highlighted that the addition of Ag-PVA beads enhanced nitrate removal and nitrogen selectivity.

Table 2: Nitrate conversion with various cathodes and their selectivity after 90min electrolysis

Cathode electrode	**Absence of Catalyst**				**Presence of catalyst**			
	NO_3-N conversion (%)	**S_{NO_2-N} (%)**	**S_{NH_3-N} (%)**	**S_{N_2-N} (%)**	**NO_3-N conversion (%)**	**S_{NO_2-N} (%)**	**S_{NH_3-N} (%)**	**S_{N_2-N} (%)**
SS	47±0.6	10.6±1.9	49.0±0.3	40.4±0.2	65±1.6	9.2±0.5	26.2±0.6	64.6±0.5
Fe	70±0.2	ND	75.7±0.4	24.3±0.4	85±0.8	1.2±0.4	37.7±0.6	62.1±0.2
Fe/Sn	21±0.4	19.1±1.1	80.9±0.9	ND	59±1.7	5.0±0.7	35.6±0.7	59.4±0.5
Cu	70±1.2	5.7±0.5	52.9±0.7	41.4±0.5	75±1.3	9.3±1.4	37.3±0.3	53.4±0.4
Ti	70±0.5	8.6±0.7	54.3±0.6	37.1±1.4	72±1.1	4.1±0.4	51.5±0.4	44.4±0.8

Conditions: NO_3-N: 25 mg/L, anode: Gr, Na_2SO_4: 2g/L as electrolyte, current density: 15 mA/cm^2, Ag-PVA: 6.67mM, reaction time: 90min

Note: To calculate the selectivity for end-products, nitrate removal (%) is considered to be 100%. ND means not detected.

Figure 14 shows the nitrate reduction and generation of nitrite-N, ammonia-N, and nitrogen-N after 90min reaction time in the absence and presence of 6.67mM Ag-PVA beads catalyst at 15mA/cm^2 current density. The extent of nitrate elimination in the absence of Ag-PVA catalyst went as follows: Fe > Ti > Cu > SS > Fe/Sn. In comparison to

Fe and Cu cathodes, Cu and Ti cathodes showed stronger selectivity towards nitrite production. When using Fe cathode, nitrite production was minimal.

The Fe cathode produced excellent results for nitrate reduction when Ag-PVA beads were present as well, whereas Fe/Sn produced the least. The nitrate removal in the presence of Ag-PVA beads followed the order: Fe > Ti > Cu > SS > Fe/Sn. The presence of the catalyst with Fe cathode resulted in the lowest conversion to nitrite along with the maximum nitrate removal, and the largest nitrogen gas conversion. Due to the serious health concerns connected with nitrite, the USEPA has set a strict limit of 1 mg/L NO_2-N. (ATSDR - Agency for Toxic Substances and Disease Registry, 2013). Thus, Fe was selected as a cathode for further research because it delivered the lowest nitrite formation and the maximum nitrogen gas selectivity in the presence of Ag-PVA beads.

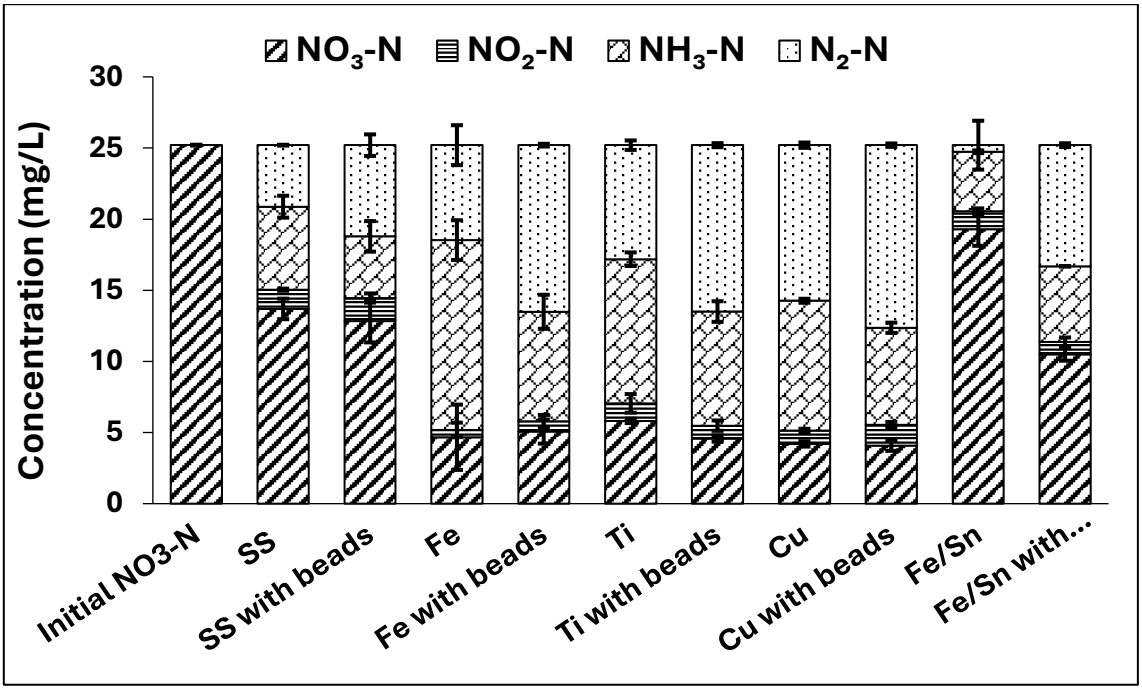

Figure 6 : Nitrate reduction using various cathode materials in absence and presence of Ag-PVA beads

(Reaction conditions: NO_3-N: 25mg/L, 6.67mM Ag-PVA beads, anode: Gr, Na_2SO_4 as electrolyte: 2g/L, current density: 15mA/cm^2, reaction time: 90min)

The published literature has findings on the impact of cathode material that are comparable to our results. For instance, employing a Ni-Cu sponge as the cathode,

Beltrame et al. (2020) reported a 44% removal of nitrate with nitrite as the primary result. Moreover, Pérez-Gallent et al., (2017) showed that the Cu cathode increased the generation of nitrite in an alkaline media during the electrocatalytic reduction of nitrate. Li et al. (2016) studied a divided cell with Al, Fe, Ni, and Cu cathodes and a Ti/TiO_2 nanotube array anode, it was discovered that Fe was the most effective cathode among them, reducing nitrate by 91% and being most selective for N_2.

4.1.3.3 Effect of current density

One of the most crucial variables in the ECR process is the current density. As seen in Figure 15 , the impact of various current densities, including 5, 10, 15, and 20mA/cm^2 in the presence of Fe cathode and Gr anode, on nitrate removal and the end-product selectivity was investigated. At current densities of 5, 10, 15, and 20 mA/cm^2, respectively, the NO_3-N removal was 74%, 80%, 86%, and 80%, while TN removal was 19, 43, 53, and 42%. Thus, %nitrate removal increased from 74 to 86% with an increase in current density from 5 to 15 mA/cm^2, and slightly decreased to 80% with further increase to 20 mA/cm^2. Moreover, the ammonia accumulation at the end of 90 min was highest at 20 mA/cm^2 current density. The nitrite generation was consistently lower than 1 mg/L, irrespective of the current density variation. According to Lan et al. (2016), when current density increases, hydrogen production at the cathode rises, inhibiting the formation of N≡N bonds and promoting the formation of N-H bonds. Consequently, a 15 mA/cm^2 current density was deemed ideal.

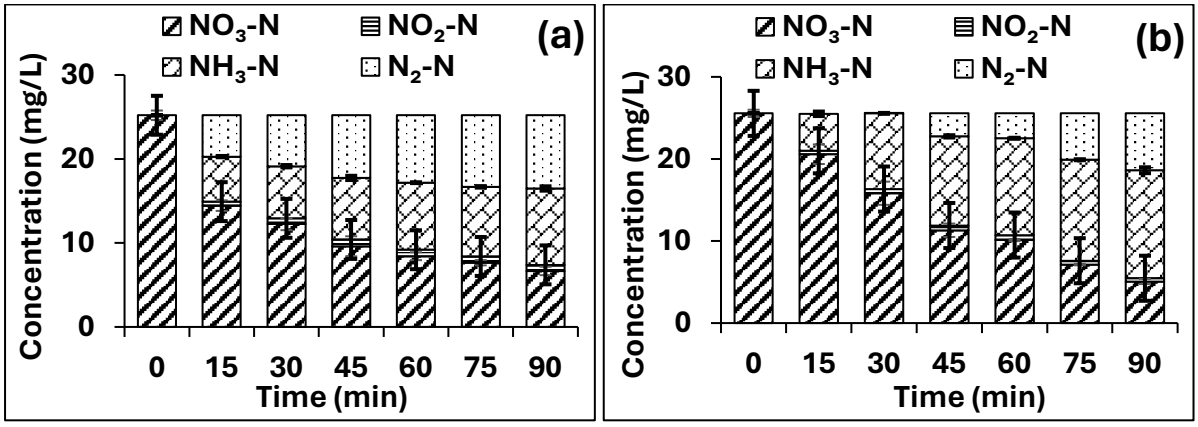

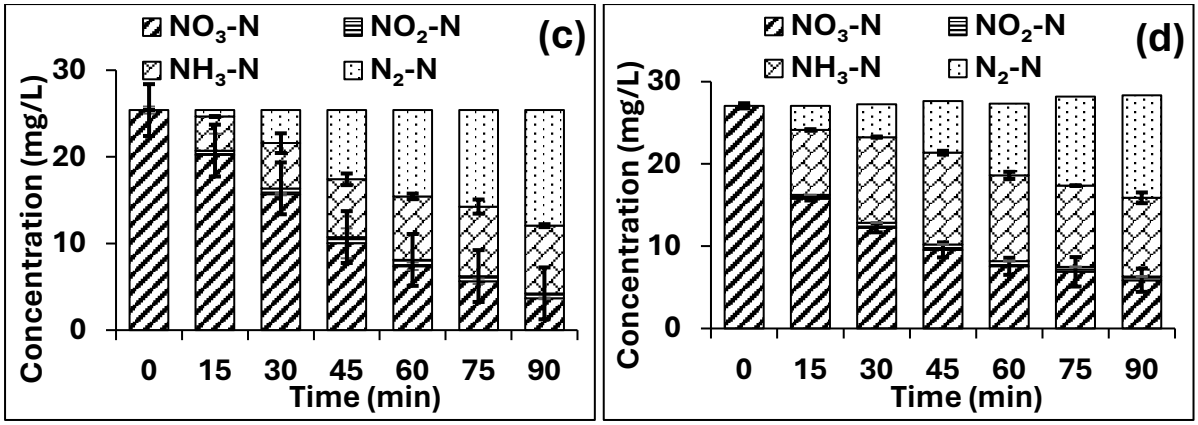

Figure 7 : Effect of current density on nitrate removal (a)5mA/cm², (b)10mA/cm², (c)15mA/cm², and (d)20mA/cm²

(Reaction conditions: NO_3-N Concentration: 25 mg/L, anode: Gr, cathode: Fe, Ag-PVA: 6.67mM, reaction time: 90 min)

A comparison of the accumulation of end-products at the end of 90 min reaction time at varying current densities is shown in Figure 16. The specific removal of NO_3-N is (mg NO_3-N removed/Ah) and current efficiency is also shown in Figure 16 as an inset. It may be seen that with increasing current density, the specific NO_3-N removal declined almost linearly, most likely due to loss of electrical energy in unfavourable reactions.

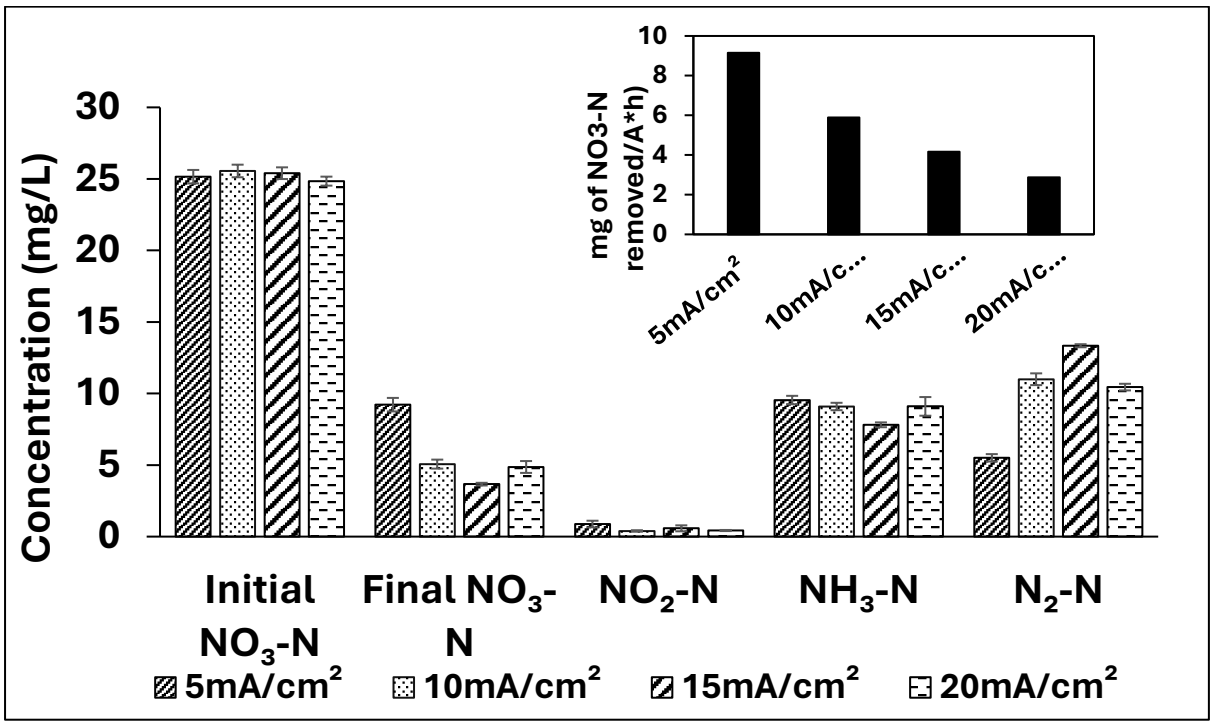

Figure 8 : Effect of current density in the presence of Ag-PVA beads. Inset figure shows specific energy consumption for nitrate removal.

(Reaction conditions: NO_3-N Concentration: 25 mg/L, anode: Gr, cathode: Fe, Ag-PVA beads: 6.67mM, reaction time: 90 min)

4.1.3.4 Effect of the initial nitrate concentration

Figure 17 shows the effects of various initial nitrate concentrations (25, 50, and 100 mg/L) assessed on the reduction of nitrate at a current density of 15 mA/cm^2 in the presence of 6.67mM Ag-PVA beads for 90 minutes of electrolysis time. The nitrate removal was more than 90% for all three initial nitrate concentrations which means it is an independent parameter. However, when the initial nitrate concentration increased, NO_2-N and NH_3-N generation also increased. Thus, the initial nitrate concentration had an impact on product selectivity. According to Su et al. (2017), the end-product selectivity may change when the starting concentration of NO_3-N increases because more electrical energy may be required to decrease NO_3-N to manufacture NH_3-N rather than H_2O to produce H_2.

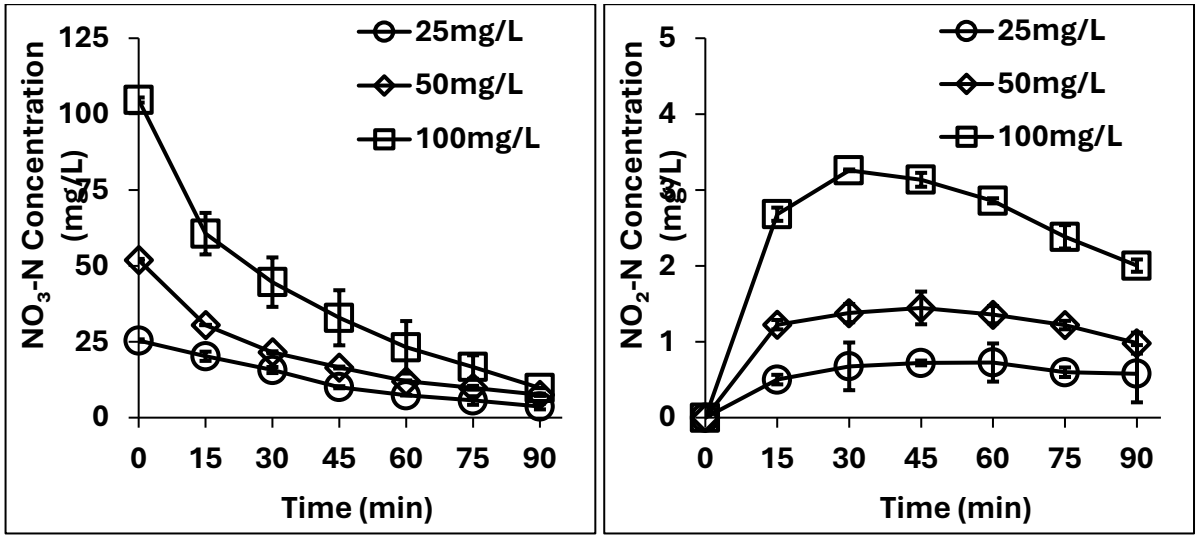

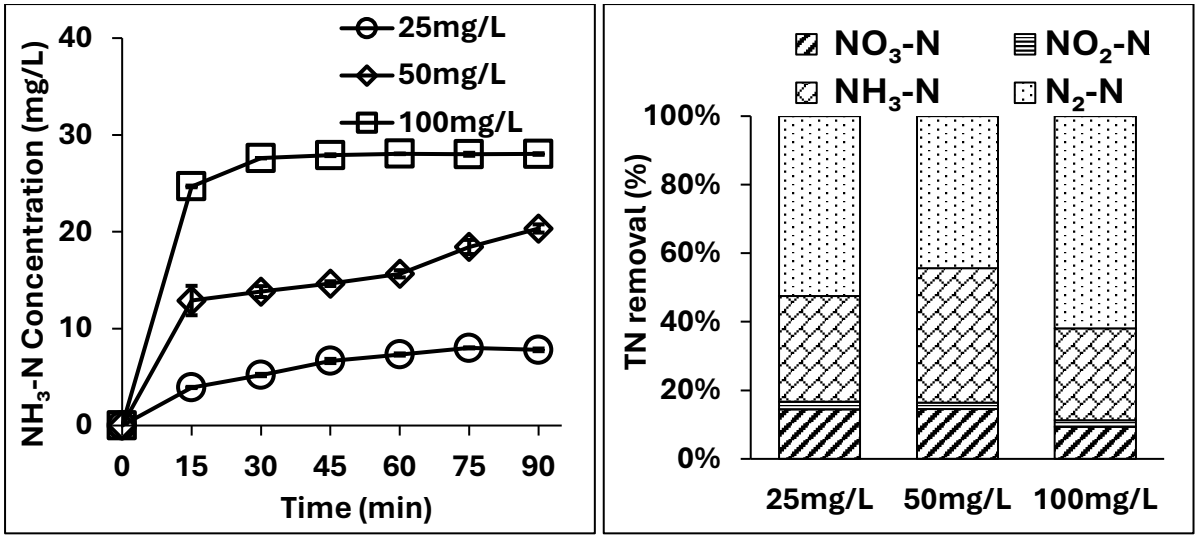

Figure 9 : Effect of initial nitrate concentration

(Reaction conditions: anode: Gr, cathode: Fe, current density: 15mA/cm^2, Ag-PVA beads: 6.67mM, reaction time: 90 min)

4.1.3.5 Reusability of Ag-PVA beads

Catalysts must be reusable to be used on a wider scale. Ag-PVA beads' capacity to be reused for NO_3-N reduction is shown in Figure 18. As can be observed, there was no discernible decline in catalytic activity after 8 consecutive reaction cycles using the Ag-PVA beads. However, after 8th cycle, nitrate reduction decreased from 86% to 78% for 9th cycle and 72% for 10th cycle. Also, it was observed that after 10 consecutive reuse, there was negligible change in NO_2-N accumulation (Figure 18b). It is interesting to note that after the eighth cycle, ammonia formation (Figure 18c) became more selective which results in decrease of TN removal (Figure 18d). Ag layer sloughing was not noticed. However, it was found that the dark brown colour of the Ag-PVA beads lightened to light brown as the number of reuses increased. This may be related to the oxidative degradation of Ag. Zhao et al. (2021) evaluated a Cu nanoparticle cathode modified with nitrogen-doped porous carbon for electrochemical removal of nitrate, and they found that the stability of cathode was for 5 cycles of the process.

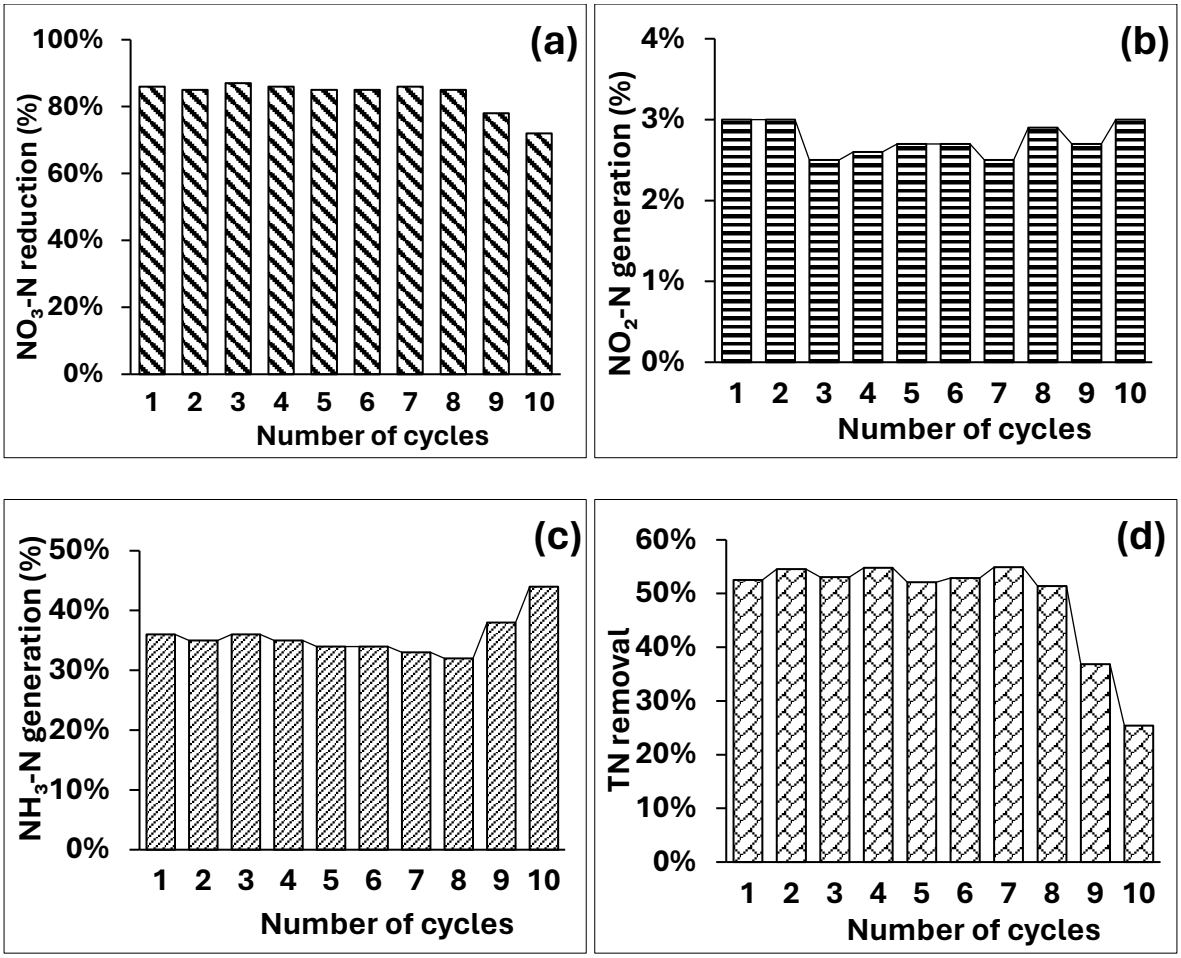

Figure 10 :Reusability of Ag-PVA beads

(Reaction condition: cathode: Fe, anode: Gr, NO_3-N: 25 mg/L, reaction time: 90 min, current density: 15 mA/cm^2, Ag-PVA: 6.67mM)

Following are the salient observations from section 4.1:

1. SEM and EDAX confirmed the proper coating of silver (Ag) on polyvinyl alcohol beads (PVA).
2. Presence of Ag-PVA beads in an undivided as well as divided cell enhanced nitrate reduction. Not only nitrate reduction, however, selectivity was also changed in the presence of a catalyst.
3. The concentration of Ag-PVA beads also played a key role in nitrate reduction.
4. Fe cathode gave prominent results among other cathode materials in the presence of a catalyst resulting in nitrogen gas as the maximum by-product.
5. Increasing current density was favourable for an increase in nitrate reduction up-to some point as further increasing changed the selectivity.
6. Increasing initial nitrate concentration gave almost similar nitrate reduction but had an impact on selectivity.

7. The reusability of Ag-PVA beads was good enough.

4.2 ECR of Nitrate using AgMPs

The morphological and crystallography study of AgMPs was conducted using SEM and XRD. In both undivided and divided cells, experiments were conducted. The findings of nitrate reduction in undivided and divided cells, as well as the impacts of different parameters in divided cell, are discussed in this section.

4.2.1 Morphological study of AgMPs

The morphological analysis of AgMPs was done by SEM. Two distinct magnifications of the SEM images of fresh and used AgMPs are shown in Figure 19. It was discovered that AgMPs of varied sizes were polydisperse. It may be seen that the AgMPs are highly aggregated particles with sizes ranging from as low as 0.05 mm (Figure 19 a and c) to as large as 0.4 mm (Figure 19 b and d).It should be observed that the morphology of fresh and used AgMPs has not significantly changed. Initially, the particles formed were in nanometre size. However, deliberately promoting the agglomeration of these nanoparticles to form larger Ag metal agglomerates that can be easily separated from the reaction medium by gravity settling. The SEM images of AgMPs used in our study (Figure 19) shows that the particle size ranges from 50 to 400 micron. We also confirmed the size of AgMPs by settling velocity calculations using Stoke's law and found that the particles were ≥30 micron in size.

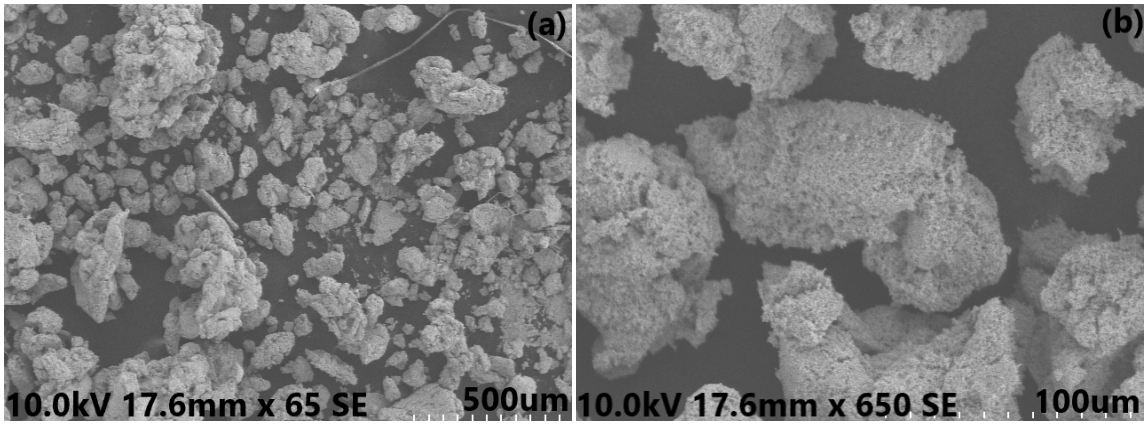

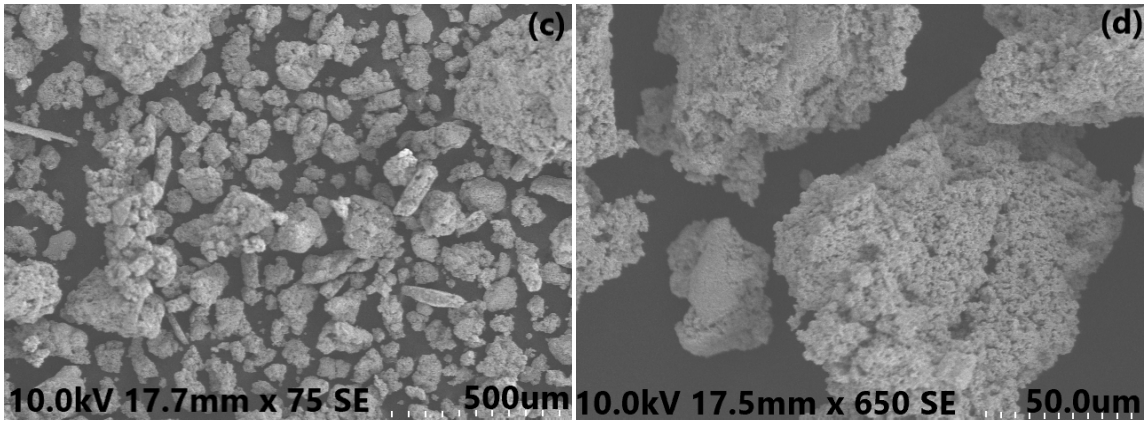

Figure 11 : SEM analysis of fresh AgMPs (a) and (b); used AgMPs (c) and (d)

4.2.2 Crystallographic study of AgMPs

The XRD analysis of both fresh and used AgMPs is shown in Figure 20. A chemical reduction procedure efficiently synthesised pure silver metal particles, according to an XRD examination. Peaks were found for both samples at 38, 44, 64, and 78 degrees, which match the facets of the crystal planes' Braggs reflections (111), (200), (220), and (311) at 2θ (degree). According to JCPDS file No. 04-0783, these peaks match the face-centred cubic (fcc) structure of silver. Additionally, tiny peaks were discovered in the examination of used AgMPs and are indicated in Figure 20 with "*". These peaks supported the creation of a minor quantity of Ag_2O in the used AgMPs, according to JCPDS file No. 12-793 and Ng et al. (2016).

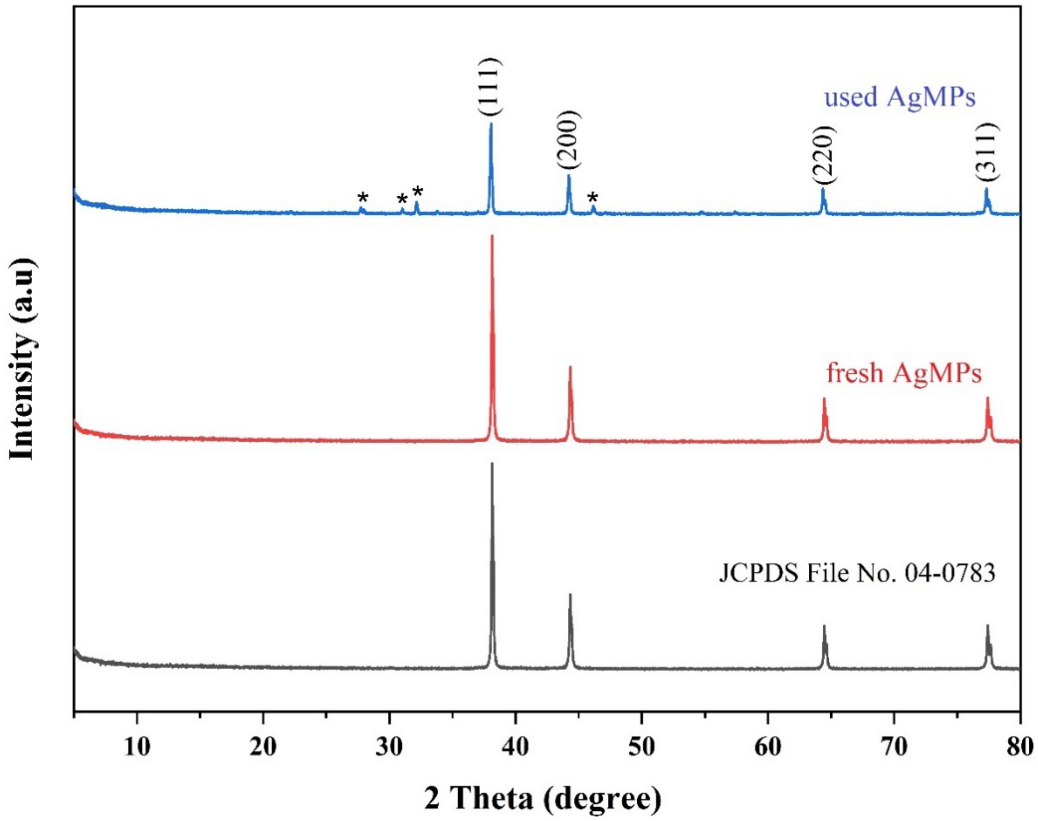

Figure 12 : XRD analysis of fresh and used AgMPs

Table 5 and 6 described the full width at half maximum (FWHM) and crystal size of fresh and used AgMPs at different angles. Since the AgMPs were required to be finely ground for XRD analysis, the size of particles depicted in Table 5 and 6 is smaller than that determined by SEM analysis. Nevertheless, it proves that AgMPs are agglomerated particles.

X-ray diffraction (XRD) was used to detect the purity, crystalline nature, and particle size of synthesized silver particles. The particle size of the fresh and used AgMPs were calculated by using Scherrer's equation (6) as follows:

$$D = \frac{K\lambda}{\beta\left(\frac{1}{2}\right) cos\,\theta} \qquad \text{Equation (6)}$$

where D is average crystallite size and β is line broadening in radians (full width at half maximum of the peak in radians). λ is wavelength of X-ray and θ is Braggs angle. K is constant

(geometric factor = 0.94)

Table 3 : Full width at half maximum (FWHM) and size calculation of fresh AgMPs

Sr. No.	2θ (degree)	d-spacing (Å)	FWHM (°)	Size (nm)
1.	38.14	2.35	0.09	91.72
2.	44.32	2.04	0.12	71.06
3.	64.45	1.44	0.11	83.81
4.	77.40	1.23	0.14	75.77
	Average			80.59

Table 4 : Full width at half maximum (FWHM) and size calculation of used AgMPs

Sr. No.	2θ (degree)	d-spacing (Å)	FWHM (°)	Size (nm)
1.	38.04	2.36	0.12	71.19
2.	44.22	2.04	0.13	65.95
3.	64.35	1.44	0.12	78.50
4.	77.30	1.23	0.14	73.02
	Average			72.2

4.2.3 Nitrate removal in an undivided cell

Figure 21 displays the outcomes of nitrate reduction in the undivided cell using a Ti cathode and a Ti/RuO_2 anode during a 120-minute electrolysis duration. In an undivided cell, the maximum amount of nitrate reduction was limited to 18% and almost entire amount of nitrate removed was transformed to NH_3-N. In the presence of 8 mM AgMPs, the nitrate reduction rose to 63%, yielding 13% NO_2-N, 35% NH_3-N, and 15% N_2-N in the undivided cell.

In the literature, similar findings have been described. Ye et al. (2020) explored nitrate reduction utilising Ti/RuO_2 and Ti mesh plates as the anode and cathode, respectively, in

the presence of cobalt-coated activated carbon particles. According to the authors, ammonia was produced as a byproduct of nitrate reduction that was oxidised on the anode. According to the published study results, undivided cell remove nitrate far less effectively than divided cell.

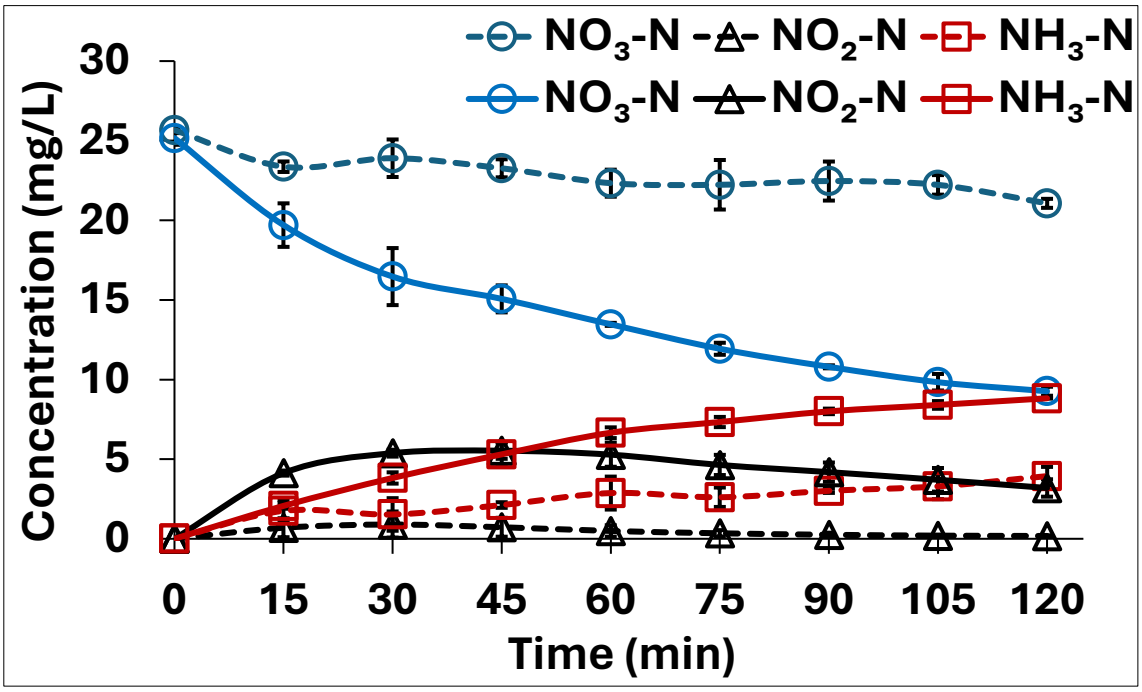

Figure 13 : NO_3-N removal in the absence (dotted line) and presence (solid line) of AgMPs in an undivided cell

(Reaction conditions: NO_3-N: 25 mg/L, cathode: Ti, anode: Ti/RuO_2, current density: 10 mA/cm^2, Na_2SO_4 as electrolyte: 2 g/L, AgMPs: 8mM, reaction time: 120 min, inter-electrode gap: 7.7 cm)

For instance, Szpyrkowicz et al. (2006) examined several reactor configurations for the electrochemical reduction of nitrate and proposed that the membrane reactor (i.e., divided cell) yields more nitrate removal than the undivided cell. Further research was conducted utilising a divided cell since the nitrate reduction process and selectivity towards N_2 in an undivided cell did not seem to be promising.

4.2.4 Nitrate removal in a divided cell

The outcomes of nitrate reduction in a divided cell using a Ti cathode and a Ti/RuO_2 anode during a 120-minute reaction period are shown in Figure 22. In the divided cell, nitrate

was reduced by 77% while NH_3-N (57.7%), NO_2-N (12.8%), and N_2-N (29.5%) were produced in the absence of AgMPs. However, in the presence of 8mM AgMPs, nitrate reduction rose to 99% and N_2-N production increased to 60%. As a result, AgMPs improved nitrate reduction as well as the selectivity for N_2-N production. The most favoured by-product of nitrate reduction, N_2-N, must be emphasised here.

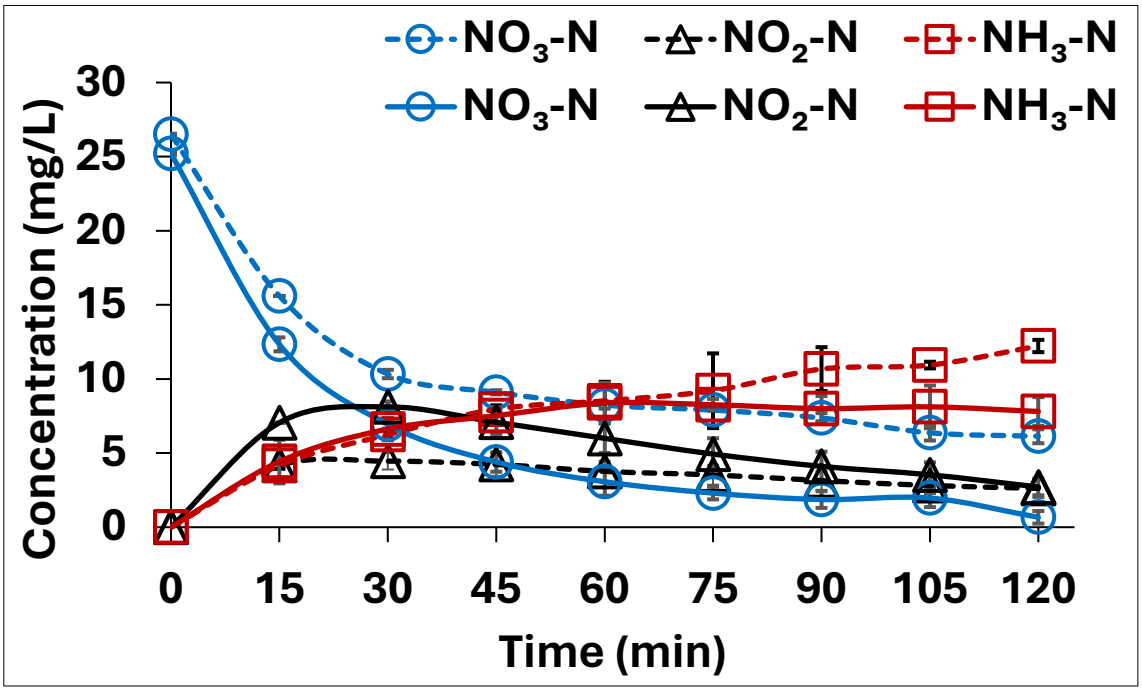

Figure 14 : NO_3-N removal in the absence (dotted line) and presence (solid line) of AgMPs in a divided cell

(Reaction conditions: NO_3-N: 25 mg/L, cathode: Ti, anode: Ti/RuO_2, current density: 10 mA/cm^2, Na_2SO_4 as electrolyte: 2 g/L, AgMPs: 8mM, reaction time: 120 min, inter-electrode gap: 7.7 cm)

As a result, experimental circumstances that encourage N_2-N formation coupled with more nitrate removal are recommended. Jonoush et al., 2020 investigated Ni foam and catalyst Ni-Fe^0@Fe_3O_4 for ECR of nitrate and reported 28.16% (Ni foam) and 90.19% (Ni-Fe^0@Fe_3O_4) nitrate removal, respectively at 5mA/cm^2 after 240min of electrolysis.

The reductive electrochemical conversion of nitrate all the way to nitrogen in the presence of silver metal catalyst is already reported. Recently, Hamam & Maiza, (2022) demonstrated electrochemical catalytic reduction of nitrate on a silver nanoparticles-polypyrrole composite film leading to the formation of nitrogen gas as the final product.

The authors further stated that Ag's strong electrical conductivity and inherent catalytic activity for nitrate reduction resulted in N_2 formation. Similarly, Couto et al. (2016) also reported the formation of N_2 during electroreduction of nitrate using a carbon fiber cathode electrodeposited with silver nanoparticles.

4.2.4.1 Effect of concentration of AgMPs

Figure 23 displays the effect of the concentration of AgMPs on nitrate removal. In a divided cell, the selectivity towards NO_2-N ($S_{NO_2\text{-}N}$), NH_3-N ($S_{NH_3\text{-}N}$), and N_2-N ($S_{N_2\text{-}N}$) is shown in Table 5 along with the effect of different catalyst concentrations on nitrate removal using Ti as cathode and Ti/RuO_2 as anode. The mass activity of the catalyst (mg NO_3-N removed per gm Ag per min) is also shown in Table 7 . It can be observed that when AgMPs concentration grew from 4 mM to 8 mM, nitrate removal increased from 83 to 99%; however, there was a little decline in nitrate removal (from 99 to 95%) as AgMPs concentration climbed further. As a result, the order of nitrate reduction for different concentrations of AgMPs was: 8mM > 10mM > 14mM > 20.8mM > 6mM > 4mM. It is notable that the catalyst concentration also affected the selectivity of the final products. With 4mM AgMPs present, $S_{N_2\text{-}N}$ and $S_{NH_3\text{-}N}$ were 32 and 44%, respectively. However, despite the mass activity being lower than that at 4 mM, the selectivity towards N_2-N (60%) was highest, while that for the NH_3-N (31%) formation was lowest, in the presence of 8mM AgMPs. This observation is similar to the one noted in the case of Ag-PVA beads. It was observed that with increasing concentration of Ag-PVA beads, the selectivity towards ammonia was increased and N_2-N decreased. As a result, 8mM AgMPs were determined to be the optimal dose for additional research. Figure 23 shows the effect of the concentration of AgMPs on the nitrate removal and the end-product formation after 120min reaction time.

Table 5: Effect of AgMPs dose on end-product selectivity and nitrate reduction

Catalyst Dose	Nitrate conversion (%)	Mass Activity (mg of NO_3-N	Concentration of NO_2-N (mg/L)	Concentration NH_3-N (mg/L)	$S_{NO_2\text{-}N}$ (%)	$S_{NH_3\text{-}N}$ (%)	$S_{N_2\text{-}N}$ (%)

		removed/ min/g Ag)					
Absence	76 ± 0.9	-	2.61	11.72	12.8±0.6	58.0±0.4	29.1±1.1
4mM	83 ± 0.5	0.411	4.78	7.24	16.0± 1.3	44.0±1.4	32.0±1.2
6mM	92±0.9	0.362	3.81	12.92	14.0± 0.2	48.0 ±0.3	38.0±0.5
8mM	99 ±1.0	0.289	2.47	7.81	10.0± 1.9	31.0±0.9	60.0±0.5
Catalyst Dose	**Nitrate conversion (%)**	**Mass Activity (mg of NO_3-N removed/ min/g Ag)**	**Concentration of NO_2-N (mg/L)**	**Concentration NH_3-N (mg/L)**	$S_{NO_2\text{-}N}$ **(%)**	$S_{NH_3\text{-}N}$ **(%)**	$S_{N_2\text{-}N}$ **(%)**
10mM	97 ± 0.7	0.227	3.87	9.04	14.4± 0.4	34.0±0.4	46.0±0.8
14mM	95 ± 1.8	0.156	4.06	8.28	17.0±0.4	35.1±1.9	47.9±1.3
20.8mM	95 ± 1.9	0.088	3.87	8.38	15.8±0.4	34.8±0.6	49.4±0.1

Reaction conditions: NO_3-N: 25 mg/L, cathode: Ti, anode: Ti/RuO_2, current density: 10 mA/cm^2, Na_2SO_4: 2g/L as an electrolyte, reaction time: 120 min, inter-electrode gap: 7.7 cm

∗ Note: To calculate the selectivity for end-products, nitrate removal (%) is considered to be 100%.

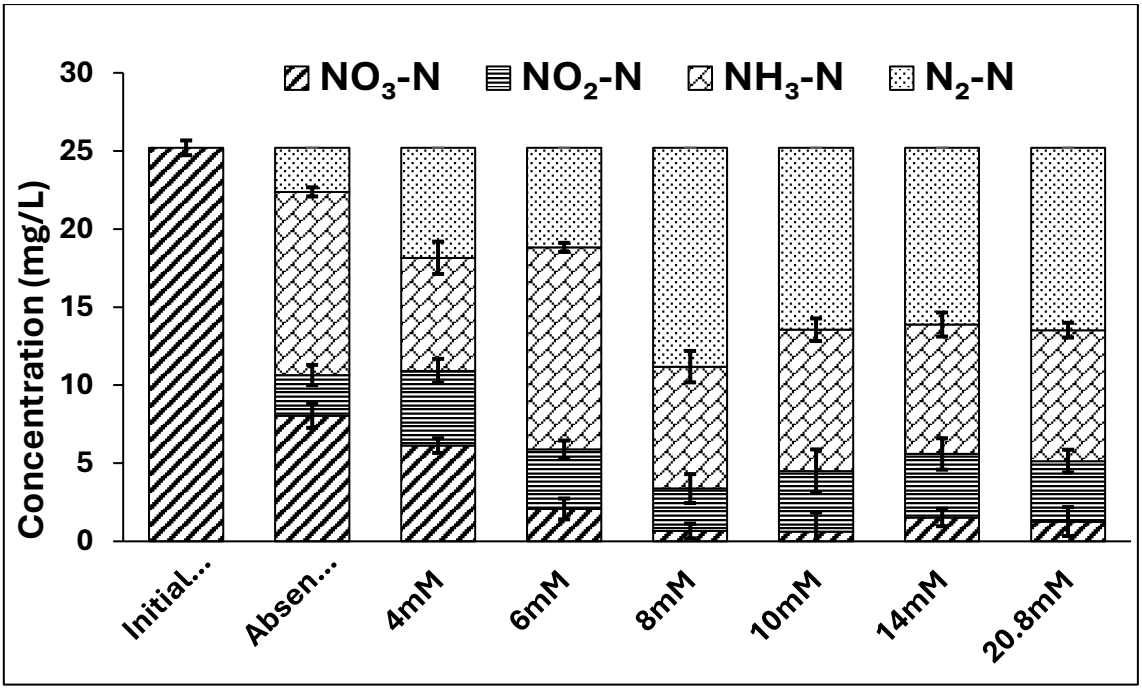

Figure 15 : Effect of various concentrations of AgMPs catalyst

(Reaction conditions: NO_3-N: 25 mg/L, cathode: Ti, anode: Ti/RuO_2, current density: 10 mA/cm^2, Na_2SO_4: 2g/L as electrolyte, reaction time: 120 min, inter-electrode gap: 7.7 cm)

To study catalytic nitrate removal, Zhang et al. (2016) employed Pd and Cu coated alumina pellets with various Pd:Cu (1:0.29, 3:0.88, 5: 1.46, and 7:2.08 mg/cm^2) concentrations. According to authors, when Pd:Cu loading rose from 1:0.29 to 3:0.88 mg/cm^2, nitrate removal increased from 55.8% to 95% in 60min reaction time. However, lower N_2 selectivity was observed as the metal concentration in catalyst increased, with ammonia as major by-product.

4.2.4.2 Effect of inter-electrode distance

Figure 24 displays nitrate removal in a divided cell using different inter-electrode spacing (3, 5.5, and 7.7 cm) in the presence of 8 mM AgMPs at the end of 120min reaction time using Ti as cathode and Ti/RuO_2 as anode. It may be noted that nitrate removal was ranging from 93-99%, irrespective of the varying inter-electrode spacing. However, the inter-electrode spacing has a considerable impact on the end-products' selectivity. Figure 24 shows that the nitrite buildup after the reaction was inversely linked to inter-electrode spacing. The greatest TN elimination and the least accumulation of nitrite

occurred at an inter-electrode gap of 7.7 cm. Therefore, 7.7 cm was found to be the ideal inter-electrode spacing for further research. The proportion of AgMPs that could be brought within the electric field between the electrodes appears to have been directly impacted by the inter-electrode distance. In other words, at an inter-electrode spacing <7.7 cm, at any time during the reaction, a part of AgMPs would be at the other side of the cathode, i.e., on the other side of the electrical field. Thus, the contribution of AgMPs to catalytic reduction of nitrate will be lesser at inter-electrode spacing <7.7 cm, affecting the end-product selectivity. The maximum possible electrode gap at which all the AgMPs could be brought under an electrical field and made accessible for nitrate reduction was 7.7 cm.

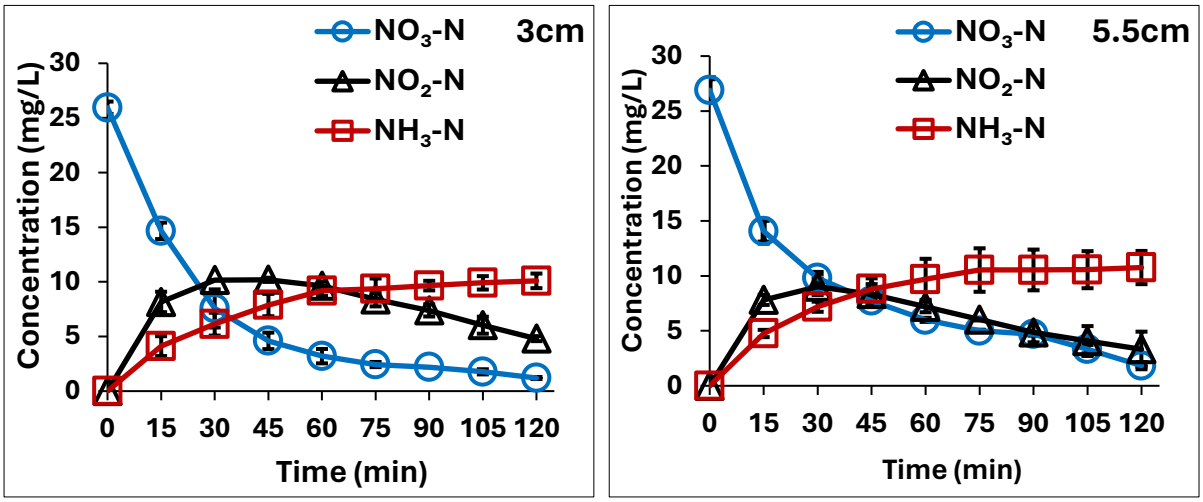

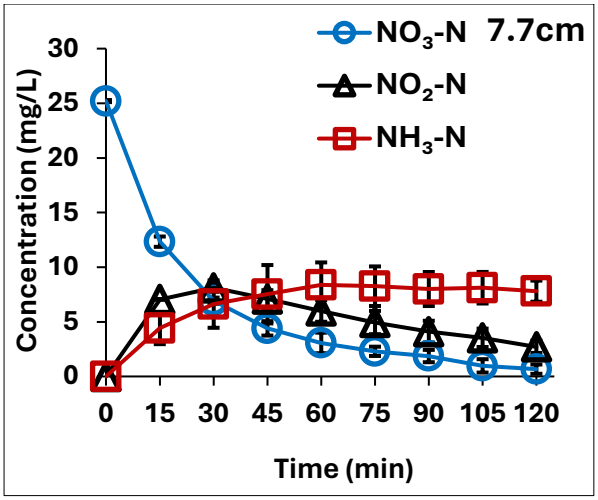

Figure 16 : Effect of inter-electrode spacing on NO_3-N elimination in a divided cell in the presence of AgMPs

(Reaction conditions: NO_3-N: 25 mg/L, anode: Ti/RuO_2, cathode: Ti, AgMPs: 8mM, Na_2SO_4 as electrolyte: 2 g/L, current density: 10 mA/cm^2, reaction time: 120 min)

4.2.4.3 Effect of the cathode material

Numerous cathode materials, including SS, Cu, Ti, Fe, and Fe/Sn, were investigated for nitrate removal. To evaluate the influence of the catalyst and the cathode material, experiments were conducted both with and without the AgMPs catalyst. Table 8 displays the conversion rate of nitrate in the absence and presence of an 8 mM AgMPs catalyst as well as their selectivity towards NO_2-N ($S_{NO_2\text{-}N}$), NH_3-N ($S_{NH_3\text{-}N}$), and N_2-N ($S_{N_2\text{-}N}$) at the end of 120 minutes of electrolysis. It is important to note that, as indicated in Table 6, both the cathode material and AgMPs affect the level of nitrate removal and the selectivity of end-products.

Table 6: The selectivity of nitrate conversion using various cathodes and their end-products

Cathode Electrode	Absence of Catalyst				Presence of catalyst			
	NO_3-N conver	$S_{NO_2\text{-}N}$ **(%)**	$S_{NH_3\text{-}N}$ **(%)**	$S_{N_2\text{-}N}$ **(%)**	**NO_3-N conversion (%)**	$S_{NO_2\text{-}N}$ **(%)**	$S_{NH_3\text{-}N}$ **(%)**	$S_{N_2\text{-}N}$ **(%)**

	sion (%)							
SS	50±0.2	6.0±0.9	57.7±1.1	36.3±0.8	88±0.3	14.6±1.2	54.2±1.1	31.2±1.7
Ti	77±1.3	12.8±0.4	57.7±0.6	29.5±0.6	99±0.1	10.0±2	31.0±1.7	60.0±0.3
Cu	74±1.6	55.0±0.4	27.9±1.0	17.0±0.6	95±0.7	8.0±0.1	50.9±0.9	41.1±1.2
Fe	73±0.9	2.3±1.2	75.8±1.6	21.9±1.8	98±0.1	1.4±0.1	51.0±0.2	47.6±0.3
Fe/Sn	25±1.1	10.7±0.8	83.0±1.4	6.3±1.4	59±0.7	6.9±0.8	54.9±1.6	38.2±0.5

Conditions: NO_3-N: 25 mg/L, anode: Ti/RuO_2, current density: 10 mA/cm^2, Na_2SO_4: 2g/L as electrolyte, 8mM AgMPs, reaction time: 120 min, inter-electrode gap: 7.7 cm

Note: To determine the selectivity for end-products, nitrate conversion (%) is assumed to be 100%.

As it can be observed, in the absence of AgMPs, nitrate was eliminated by different cathode materials in the following order: Ti > Cu > Fe > SS > Fe/Sn. Nitrate removal from Ti, Cu, and Fe cathodes was comparable; however, the main conversion was into N_2-N, NO_2-N, and NH_3-N, respectively. On the other hand, nitrate removal occurred in the presence of AgMPs in the order Ti > Fe > Cu > SS > Fe/Sn. In this case, as well, nitrate was eliminated by >95% using Ti, Cu, and Fe cathodes, however, the main transformation was into N_2-N, NH_3-N, and NH_3-N, respectively. AgMPs changed the selectivity of final products as a result. This observation is similar to the one noted in the case of Ag-PVA beads i.e., the presence of Ag-PVA beads changed the final selectivity from ammonia to N_2-N. Figure 25 displays the effect of cathode material in the absence and presence of AgMPs.

Cu cathode, interestingly, produced the highest conversion to nitrite and ammonia, respectively, in the presence and absence of AgMPs. In the published literature, higher nitrate-to-nitrite conversion employing Cu cathode in the absence of any catalyst is observed (Reyter et al., 2011; C. Roy et al., 2016). Cu and Polypyrrole coated Cu (PPy/Cu) electrodes were tested by Çirmi et al. (2015) for the removal of nitrate, and they observed the highest conversion to nitrite using Cu cathode and to ammonia using PPy/Cu cathode. According to reports, nitrate ions may readily bind to the Cu cathode and then

undergo a direct electron transfer to form nitrite. Also, using Cu cathode in the absence and presence of Ag-PVA beads, gave maximum conversion to nitrite and ammonia. However, when a catalyst is present, ammonia synthesis is facilitated by two processes: (1) the adsorption of an available proton in the solution on the catalyst, and (2) the reduction of the proton via electron transfer to yield atomic hydrogen (H_{ads}) which combines with reduced nitrogen to form ammonia. Figure 25 shows nitrate reduction in the absence and presence of 8mM AgMPs catalyst with the use of various cathode materials at 10mA/cm^2 current density for 120min reaction time.

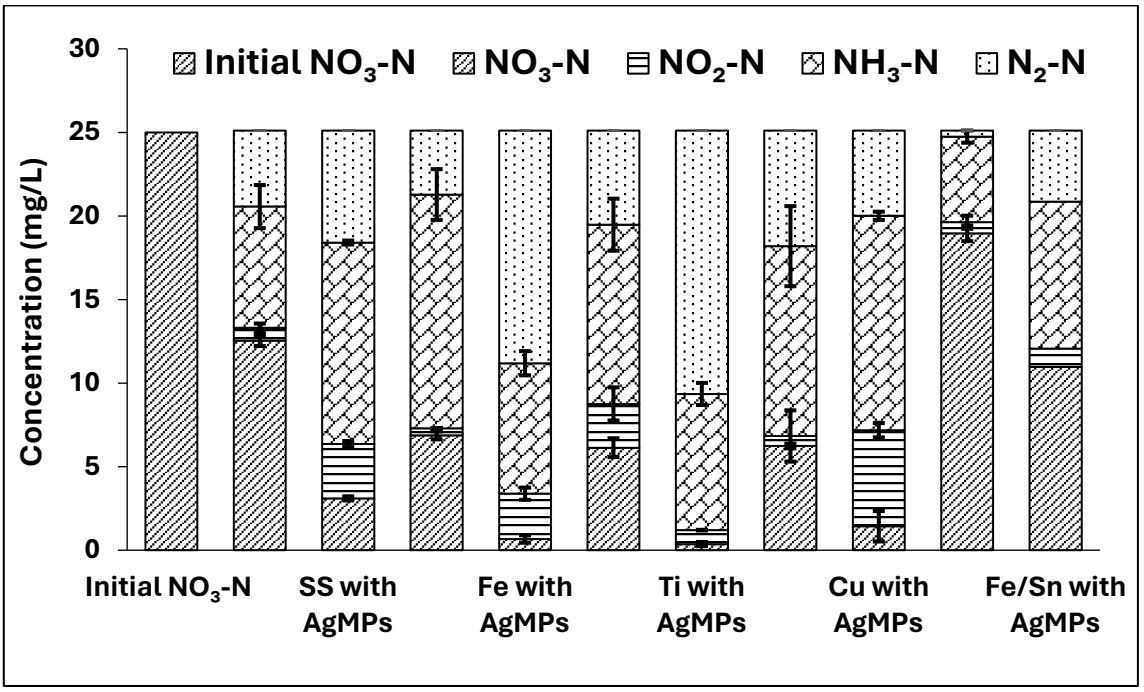

Figure 17 : Nitrate reduction using various cathode materials in the absence and presence of AgMPs

(Reaction conditions: NO_3-N: 25 mg/L, anode: Ti/RuO_2, AgMPs: 8mM, Na_2SO_4 as electrolyte: 2 g/L, current density: 10 mA/cm^2, reaction time: 120 min)

Fe and Ti cathodes are similar in their ability to reduce nitrate in the presence of AgMPs, however, Ti has a stronger selectivity towards N_2-N (60%) than Fe (47.6%). Fe is also more quickly corroded in both alkaline and acidic pH settings, which reduces the stability of Fe electrodes (Garcia-Segura et al., 2018). Ti cathode was therefore employed for further research. It is well-known that Ti's intrinsic hydrogen evolution reaction (HER) activity is

low (T. Zhang et al., 2021). In other words, the hydrogen evolution on Ti as a cathode is less. This lower hydrogen evaluation is beneficial for the electroreduction of nitrate as it reduces the competition between the evolution of hydrogen and the reduction of nitrate ions on the cathode. As a result, more electrons can be channelled for the nitrate reduction pathway, leading to the highest formation of N_2 as the final product.

4.2.4.4 Effect of current density

Current density is one of the elements that have the most impact on the electrochemical reduction process of nitrate. Studies on current densities of 5, 10, and 15 mA/cm^2 were conducted to assess the impact on the selectivity for the end-products and nitrate removal using Ti as cathode and Ti/RuO_2 as anode. As seen in Figure 26, NO_3-N removal was 90, 99, and 93% at current densities of 5, 10, and 15mA/cm^2, respectively, whereas TN removal was 30%, 60%, and 41%. As a result, when the current density was increased from 5 to 10 mA/cm^2, the nitrate reduction rose along with an increase in N_2-N generation. Nitrite generation peaked at a current density of 5 mA/cm^2 (21%) and subsequently decreased to negligible levels as the current density increased to 10 mA/cm^2. Additionally, Figure 26 displays mg NO_3-N eliminated every amp-hour. Due to side reactions, the energy needed to remove NO_3-N rises linearly with the current density.

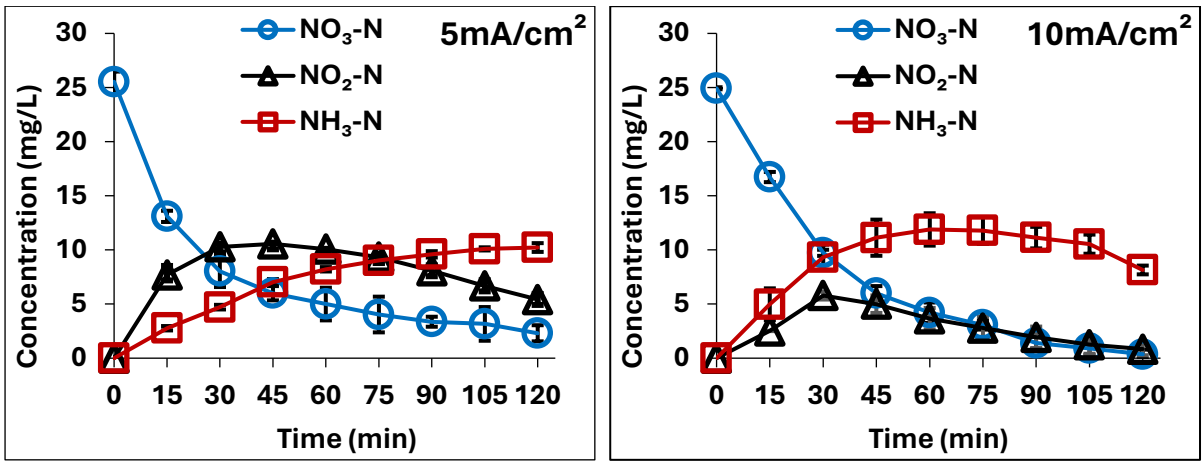

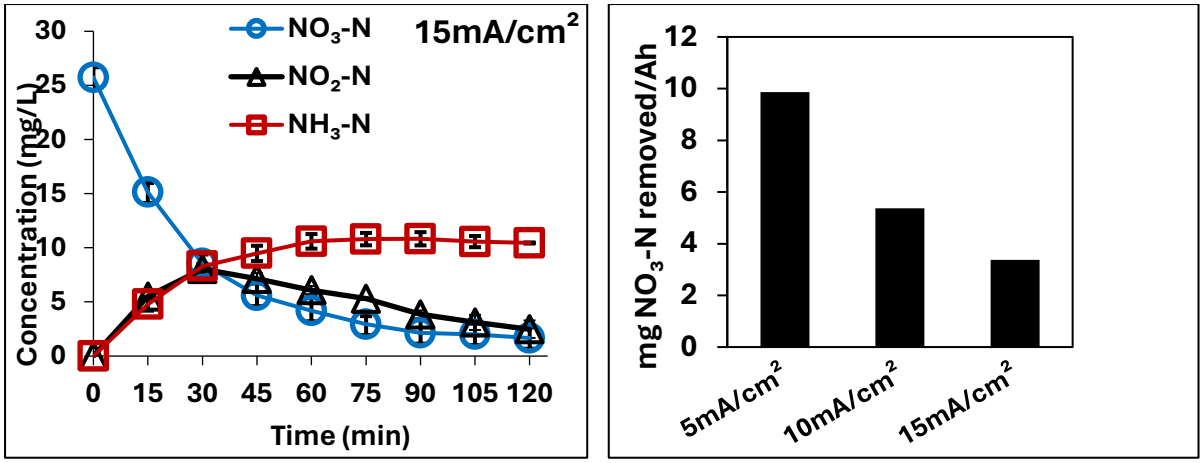

Figure 18 : Effects of current density on nitrate removal and selectivity of end-products

(Reaction Conditions: NO_3-N Concentration: 25 mg/L, cathode: Ti, anode: Ti/RuO_2, catalyst concentration: 8mM AgMPs, reaction time: 120 min; inter-electrode distance: 7.7cm)

It was found that the reduction of nitrate marginally fell to 93% with increasing selectivity in favour of ammonia generation as the current density was raised to 15 mA/cm^2. This observation is similar to the one noted in the case of Ag-PVA under similar experimental conditions. Li et al. (2016) hypothesised that when current density increased, more hydrogen was produced, promoting the combination of N-H, and discouraging the formation of N≡N, which boosts the creation of ammonia. On the other hand, Sahu et al. (2014) suggested that when the current density was too low, it was challenging to completely convert nitrate to nitrogen. Additionally, even if nitrate removal is boosted by increasing current density, an excessive amount of current density causes the electrocatalytic system to use more energy. So, it was decided that 10 mA/cm^2 current density was optimal.

4.2.4.5 Effect of initial nitrate concentration

According to the nitrate reduction mechanism stated by Chauhan & Srivastava (2022) and Zou et al. (2021), the process is highly dependent on the initial nitrate concentration. On the reduction of nitrate at a current density of 10mA/cm^2 in the presence of 8mM AgMPs for 120min of electrolysis time using Ti as cathode and Ti/RuO_2 as anode, the effects of different initial concentrations (25, 50, and 100 mg/L NO_3-N) were evaluated as depicted in Figure 27. It may be observed that with an increase in the initial nitrate

concentration, the formation and accumulation of NO_2-N and NH_3-N increased, with corresponding decrease in the formation of N_2-N. Thus, nitrate removal and product selectivity were influenced by the initial nitrate concentration. A similar observation was obtained with Ag-PVA beads that is as initial nitrate-N concentration increases, change in selectivity occurs.

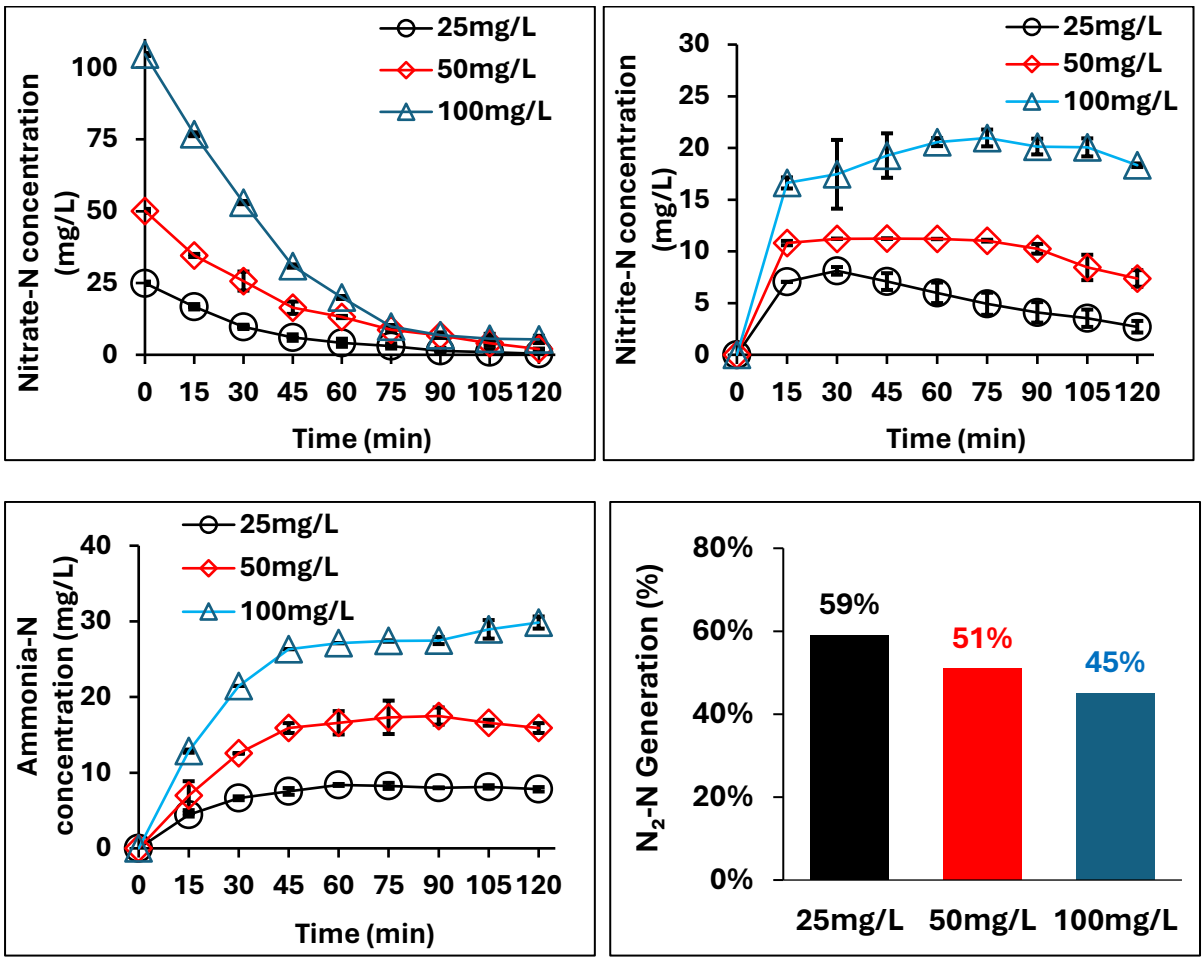

Figure 19 : Effect of initial NO_3-N concentration on nitrate reduction and its selectivity

(Reaction Conditions: cathode: Ti, anode: Ti/RuO_2, catalyst concentration: 8mM AgMPs, current density: 10mA/cm^2; reaction time: 120 min)

Table 9 shows the first-order nitrate removal rate constant values at varying initial nitrate concentrations. The first-order nitrate removal rate constant values decreased with increase in the initial nitrate concentration. According to Li et al. (2016), the cathode's restricted ability to adsorb nitrate ions as well as competition from other ions and byproducts such as nitrite and ammonia may cause the nitrate removal rate to decrease

as the nitrate concentration increases. Additionally, when the initial nitrate concentration increases, the cation exchange membrane in the divided cell is more prone to corrosion and clogging, which results in a slower rate of nitrate removal. According to Su et al. (2017), when the starting concentration of NO_3-N increases, more electrical energy may be required to decrease NO_3-N to manufacture NH_3-N instead of H_2O to produce H_2, changing the end-product selectivity.

Table 7: Effect of the initial nitrate concentration on 1st-order removal rate constant and nitrate removal efficiency

Initial NO_3-N concentration (mg/L)	1st-order Rate constant (min^{-1})	R^2	NO_3-N reduction efficiency (%)
25	0.0322	0.9945	99
50	0.0247	0.9918	96
100	0.0220	0.9908	94

(Reaction Conditions: cathode: Ti, anode: Ti/RuO_2, catalyst concentration: 8mM AgMPs, current density: 10mA/cm^2; reaction time: 120 min)

4.2.4.6 Simultaneous nitrate reduction-ammonia oxidation for TN removal

In a divided cell, while the electrical energy is fruitfully used for reduction of a target pollutant in the cathode compartment, the energy in the anode compartment is lost without any useful outcome. Therefore, the experiments were conducted by filling the catholyte of an ECR experiment (containing residual concentrations of mainly ammonia, and small concentrations of nitrate and nitrite) in the anode compartment rather than a plane sodium sulfate solution as an anolyte. Such an arrangement will provide an advantage of simultaneous reduction of nitrate in the cathode compartment and the oxidation of ammonia in the anode compartment. Figure 28 demonstrates the scheme and results of simultaneous nitrate reduction-ammonia oxidation experiments. In the 1st experiment, the fresh catholyte contained 25mg/L NO_3-N and 2g/L Na_2SO_4, and the anolyte was a 2g/L Na_2SO_4 in DI water. Ti acted as a cathode and Ti/RuO_2 acted as an anode in the presence of 8mM AgMPs in cathode compartment at 10mA/cm^2 current density in all the experiments. The results obtained in the catholyte were: NO_3-N

reduction was ≈99% with 32.9% NH_3-N and 64% N_2-N generation. In 2nd experiment, the catholyte was a fresh 25mg/L NO_3-N solution and 2g/L Na_2SO_4, and the catholyte of the first experiment containing residual ammonia was taken as anolyte. The results obtained were that NO_3-N reduction was like the 1st experiment i.e., ≈99%, however, the concentration of NH_3-N in the catholyte was increased to 60% and N_2-N concentration was decreased to 25%. On the other hand, ammonia was almost eliminated from the anolyte. This experiment cycle was continued to determine the fate of ammonia. For the 3rd experiment, again a fresh 25mg/L NO_3-N solution was as catholyte and the catholyte of 2nd experiment was taken as anolyte. The results obtained in the 3rd experiment were that NH_3-N concentration was again increased (75%) and N_2-N concentration decreased (5%) in the catholyte, with almost complete removal of ammonia in the anolyte. We performed the mass balance of ammonia for each experiment and found that the mass of ammonia eliminated from the anode compartment was almost like the mass of ammonia increased in the catholyte. In other words, there was no oxidation of ammonia in the anode compartment. It may be easily understood that under acidic conditions in the anode compartment (due to evolution of oxygen gas and accumulation of hydrogen ions), the ammonia will exist as NH_4^+ ions which facilely pass through the cationic exchange membrane to the negatively charged cathode, leading to a constant buildup of ammonia in the catholyte.

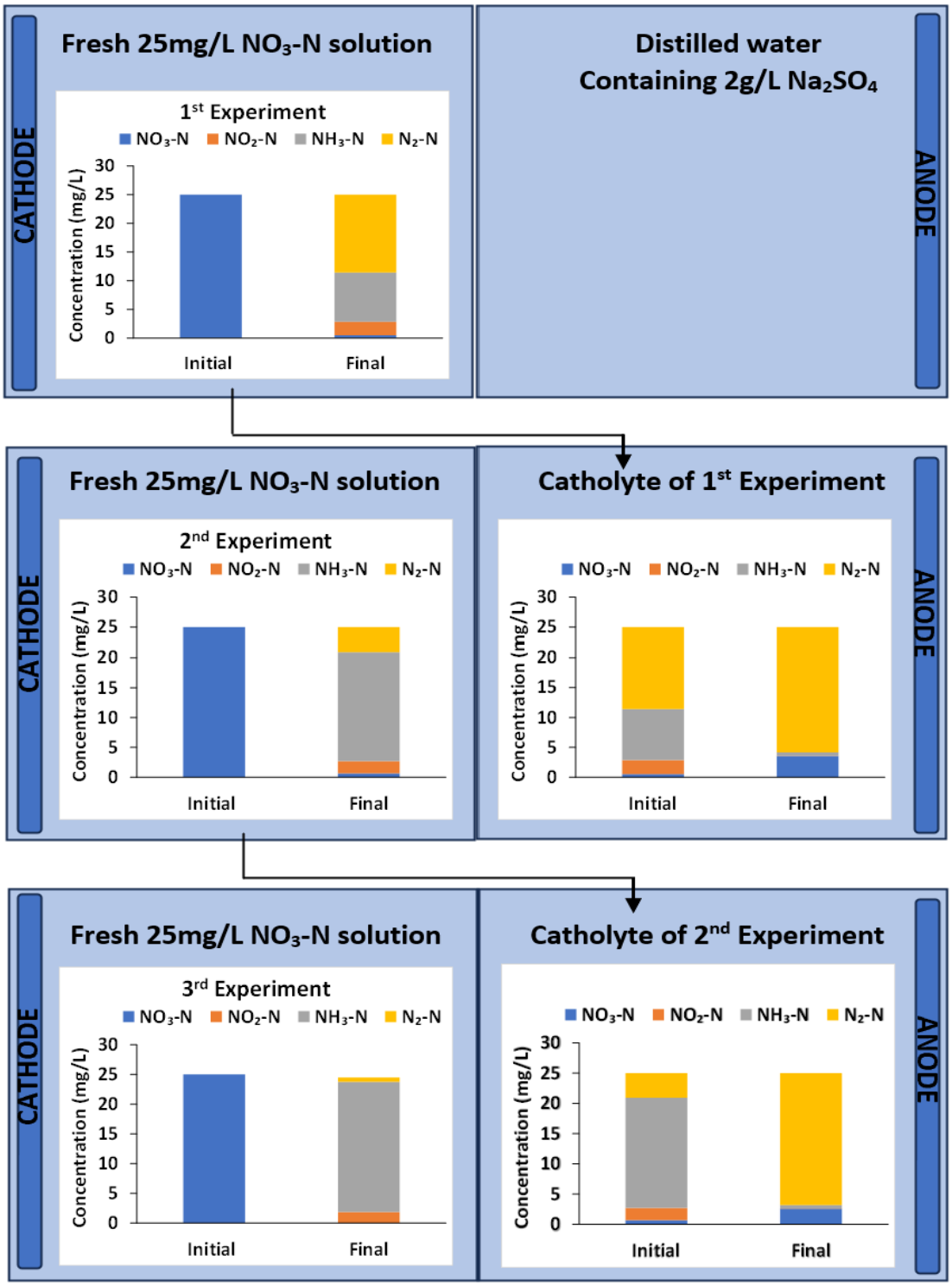

Figure 20 : Experiments and results of simultaneous nitrate removal and ammonia oxidation

4.2.4.7 Reusability of AgMPs

Only reusable catalysts may be employed on a wider scale. Figure 29 depicts the ability of AgMPs to be recycled for NO_3-N reduction. Even after 10 consecutive cycles of use,

the AgMPs' catalytic activity for nitrate removal was almost unchanged. It was interesting to see that after the third reuse, TN elimination decreased and NO_2-N build-up slightly increased. It may be noted that at the end of each reusability experiment, the AgMPs were separated by settling, washed, and reused for the next experiment. During these repeated cycles of separation and washing, some particles are inadvertently lost. When we noticed change in selectivity of end-products, after the 6th use, we measured the dry mass of AgMPs and noted ≈10% reduction in mass as compared to the original mass employed in the 1st use. Thus, we added fresh AgMPs (~0.013 g) to restore the original mass. It may be seen that the initial selectivity towards N_2 and nitrite generation and TN elimination was restored after the addition of lost AgMPs mass after the sixth cycle. Thus, the AgMPs could be reused at least ten times. It may be possible that silver metal may dissolved in the catholyte. We measured the concentration of aqueous silver ions in the catholyte solution following several re-uses. The concentration of aqueous silver ions was around 0.08 mg/L, which is significantly below the requirements for drinking water in India (IS 10500). Santos et al. (2020) employed a Pd-Cu-loaded carbon nanotube as a catalyst for the reduction of nitrate and reported that the catalyst could be reused 5 times; however, selectivity towards ammonia generation increased with repeated usage. As demonstrated by Popli & Patel (2017), RB5 dye was electrochemically reduced using silver nanoparticles three times.

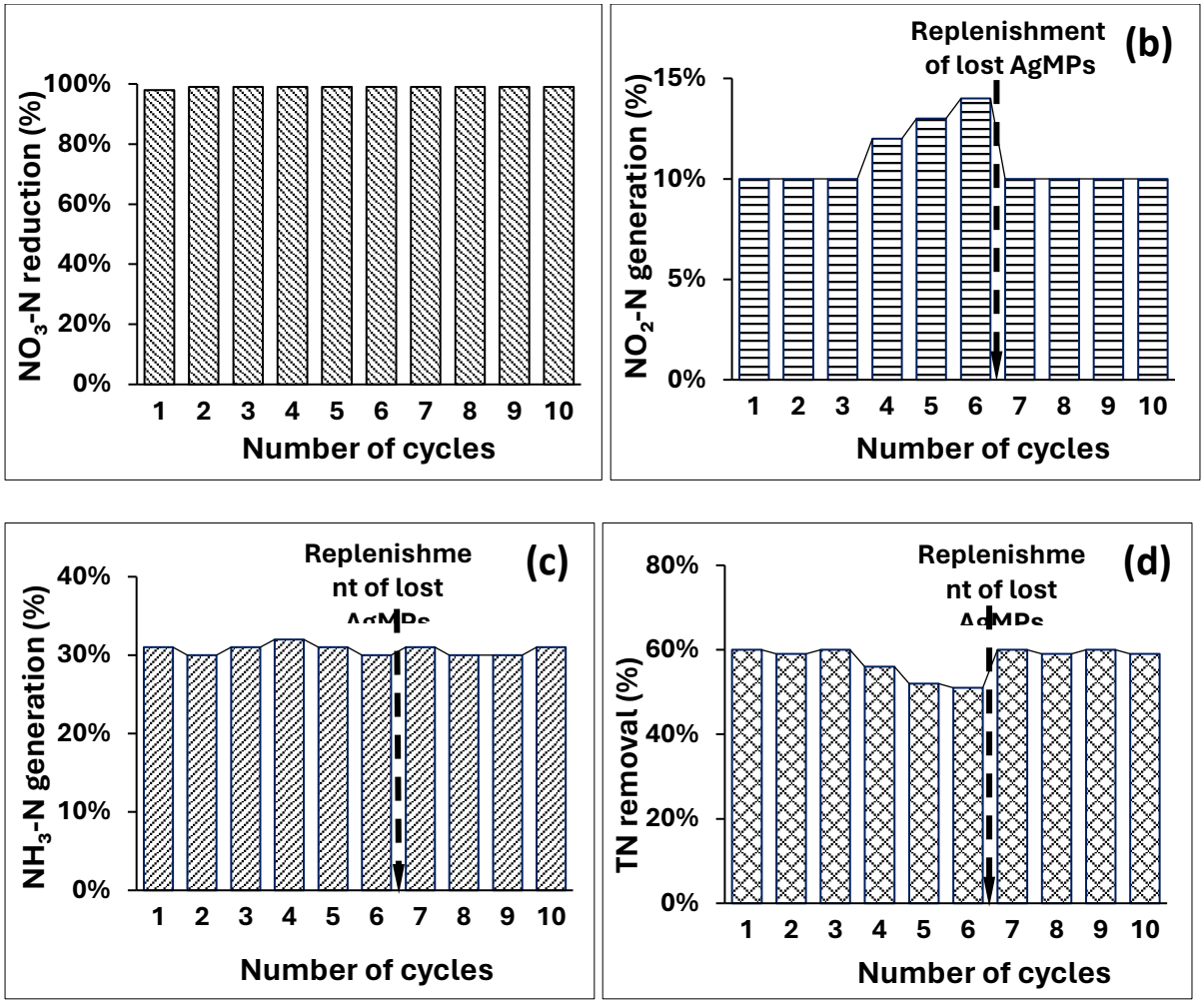

Figure 21: Reusability of AgMPs (a) nitrate reduction, (b) nitrite generation, (c) ammonia generation, and (d) TN removal

(Reaction condition: NO_3-N: 25 mg/L, cathode: Ti, anode: Ti/RuO_2, current density: 10 mA/cm^2, reaction time: 120 min, Na_2SO_4: 2g/L, catalyst concentration: 8mM AgMPs, inter-electrode distance:7.7cm)

Following are the salient observations from section 4.2:

1. SEM and XRD confirmed the proper synthesis of silver metal particles (AgMPs).
2. Nitrate reduction was boosted by the presence of an AgMPs catalyst in both undivided and divided cells. In the presence of the catalyst, the selectivity for N_2 generation is significantly improved.
3. The highest selectivity for N_2-N formation and nitrate removal was observed when Ti was used as the cathode.

4. As the current density increased (5 to 10mA/cm^2), nitrate reduction also increased. Further increasing current density (10 to 15mA/cm^2), affected the selectivity.

5. Increasing the initial concentration of nitrate resulted in a similar nitrate removal, although the selectivity of end-products was significantly impacted.

6. Reusability of AgMPs was very good with negligible solubility of Ag in treated water.

4.3 Mechanism of catalytic electrochemical nitrate removal in the presence of a spatially suspended silver catalyst

Equations 1-9 state that the principal quasi-stable intermediate generated by electrochemical reduction, before being completely reduced to ammonia or nitrogen gas, is nitrite (Garcia-Segura et al., 2018; Koparal & Öütveren, 2002). Both ammonia (NH_3) and nitrogen (N_2) are thermodynamically the most stable forms of nitrogen (Zeng et al., 2020). The conversion of nitrate (NO_3^-) to nitrite (NO_2^-) (Equations 1-4) and the conversion of nitrite (NO_2^-) to ammonia (NH_3)/nitrogen (N_2) (Equations 5-9) are the two steps that separate the reduction of nitrate (NO_3^-).

$NO_3^- + 2H^+ + 2e^- \rightarrow NO_2^- + H_2O$ (1)

$NO_3^- + e^- \rightarrow NO_3^{2-}$ (2)

$NO_3^{2-} + H_2O \rightarrow NO_2\bullet + 2OH^-$ (3)

$NO_2\bullet + e^- \rightarrow NO_2^- + 2H_2O$ (4)

$NO_2^- + 8H^+ + 6e^- \rightarrow NH_4^+ + 2H_2O$ (5)

$NO_2^- + e^- \rightarrow NO_2^{2-}$ (6)

$NO_2^{2-} + H_2O \rightarrow NO + 2OH^-$ (7)

$NO + 2H^+ + 2e^- \rightarrow N + H_2O$ (8)

$N + N \rightarrow N_2$ (9)

There may be two reaction pathways that contribute simultaneously to the reduction of nitrate in the cathode compartment in an electrocatalytic process using a divided cell: (1) nitrate reduction by catalytic hydrogenation, and (2) direct nitrate reduction on the cathode (Hôrold et al., 1993; Z. Zhang et al., 2016).

In the absence of a spatially suspended catalyst, the process of nitrate ion adsorption on the cathode, which is necessary for nitrite production, is sluggish and severely impacted by interference from other anions (Tong et al., 2017). On the other hand, the spatially dispersed catalyst (such as Ag-PVA and AgMPs) in the cathode chamber serve as micro-cathodes which offers a much greater surface area for nitrate adsorption leading to enhanced nitrate removal. Moreover, proton reduction on these Ag micro-cathodes results in the formation of nascent hydrogen, which is intercalated in Ag^0 to create highly reductive AgH_x species, as suggested in Equations 10-12, that may reduce nitrate.

$$NO_3^- + AgH_x \rightarrow NO_2^- + H_2O + Ag^0 \quad (10)$$

$$NO_2^- + AgH_x \rightarrow 0.5N_2 + OH^- + H_2O + Ag^0 \quad (11)$$

$$NO_2^- + AgH_x \rightarrow NH_3 + OH^- + H_2O + Ag^0 \quad (12)$$

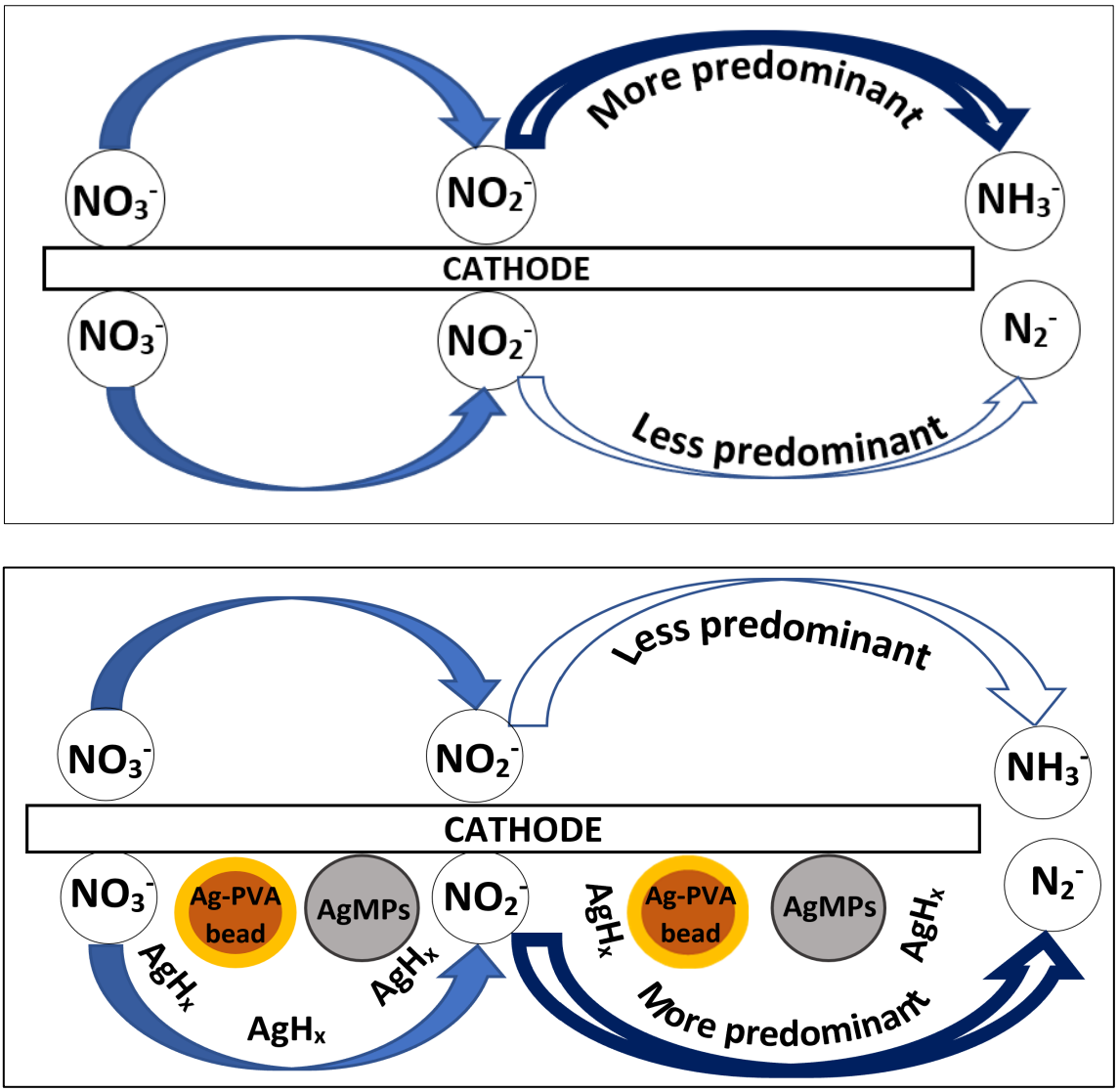

Figure 22 : Mechanism of nitrate reduction on the cathode in the absence and presence of Ag-PVA beads and AgMPs

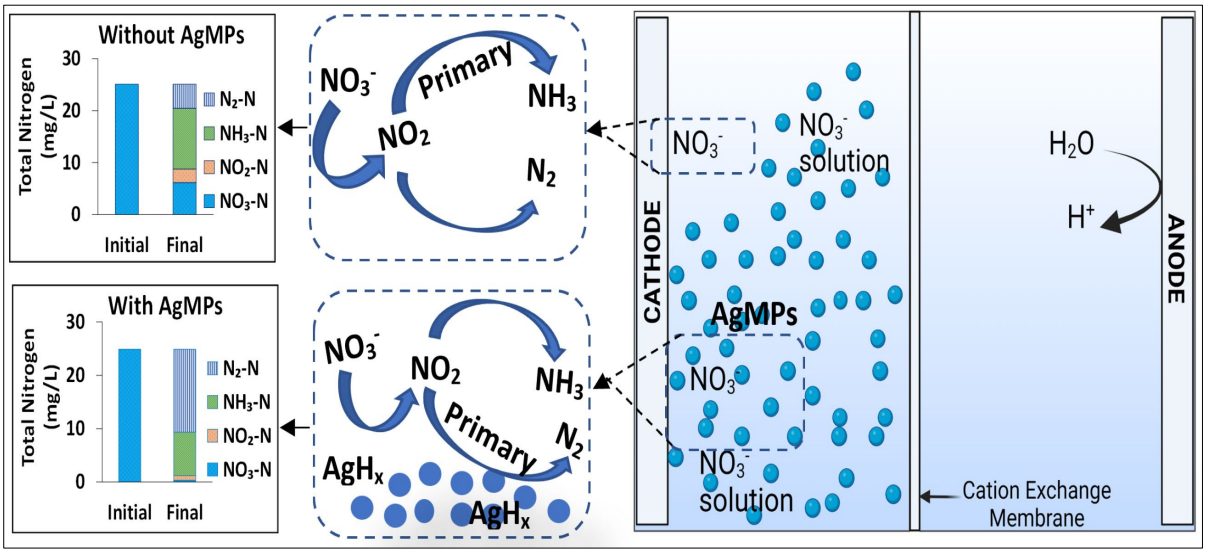

Figure 23 : Mechanism of nitrate reduction on the cathode in the absence and presence of AgMPs

Based on the description above, Figure 30 and Figure 31 visually illustrate a nitrate removal method in both the presence and absence of Ag-PVA beads and AgMPs. The formation of AgHx is already reported (Baba et al., 2001). It has already been shown that AgH_x may be used to reductively degrade aquatic contaminants (Ingle & Patel, 2022; U. D. Patel & Suresh, 2008; U. Patel & Suresh, 2006; S. Popli & Patel, 2017). As a result, AgHx species also contribute to nitrate reduction in addition to the direct reduction on the cathode, resulting in improved removal. Additionally, the AgHx species modify the selectivity of finished products. The outcomes showed that the addition of a spatially suspended catalyst increased the selectivity towards N_2.

4.4 ECR of nitrate in groundwater using spatially suspended catalyst

The ECR of nitrate in groundwater was investigated using a spatially suspended catalyst at optimised conditions. Table 10 provides descriptions of the characteristics of groundwater.

Table 8 : Characteristics of Groundwater

Parameters	Values
Nitrate-N	15 mg/L
Sulphates	8 mg/L
Chlorides	150 mg/L
Carbonates	75 mg/L
Bicarbonates	125 mg/L
pH	6.5-7.6

Figure 32 displays the nitrate-N reduction in a divided cell in the absence and presence of 6.67mM Ag-PVA beads after 90 minutes of electrolysis at a current density of 15mA/cm^2. It was discovered that the presence of a catalyst improved nitrate removal in groundwater and altered selectivity as well. In the presence of Ag-PVA beads, the reduction of nitrate increased from 53% to 85%. In the presence of the catalyst, NO_2-N

(3%), NH_3-N (57%) and N_2-N (24%) were, as opposed to 53% of NO_2-N, 52% of NH_3-N, and zero N_2-N generation in the absence of the catalyst.

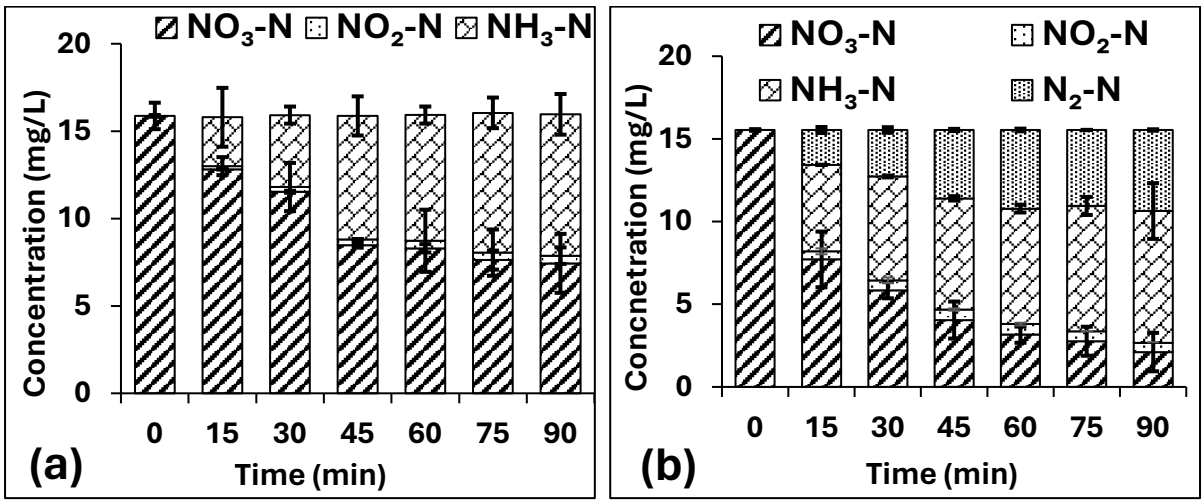

Figure 24 : Nitrate removal in the absence (a) and presence of Ag-PVA (b) beads in groundwater

(Reaction condition: Groundwater, cathode: Fe, anode: Gr, current density: 15 mA/cm^2, reaction time: 90 min, Ag-PVA: 6.67mM)

The nitrate reduction in a divided cell with the absence and presence of 8mM Ag-MPs is shown in Figure 30 after 120 minutes of electrolysis at a current density of 10mA/cm^2. It was found that catalyst presence enhanced the removal of nitrate from groundwater and changed the selectivity also. 24% of nitrate-N was reduced in the absence of a catalyst which rose to 59% in the presence of a catalyst. In the absence of a catalyst, the selectivity for NO_2-N and NH_3-N was 9.5 and 13.7%, respectively while no N_2-N generation was noted. In the presence of AgMPs, NO_2-N generation was negligible, and NH_3-N and N_2-N generation was 24 and 34%, respectively. Comparison of results depicted in Figure 32 and Figure 33 with the nitrate removal results obtained in the synthetic solution shows that the performance of both Ag-PVA and AgMPs is adversely affected in the real groundwater. Additionally, the selectivity of end-products was also severely affected as indicated by a significant decrease in N_2-N production. One of the reasons for the inferior performance of ECR in the presence of suspended catalysts in groundwater could be the competition for the adsorption of nitrate with other anions.

Moreover, silver metal is known to corrode in the presence of chloride ions forming AgCl (Ha & Payer, 2011; Park et al., 2023) which will abate the access of reactants to Ag metal. It is also important to note that under the optimum conditions the performance of Ag-PVA is better than AgMPs for nitrate removal from groundwater. This is exactly opposite to what observed in the synthetic nitrate solution wherein, the performance of AgMPs was better than Ag-PVA. It seems that polyvinyl alcohol (PVA) support may resist the deactivation of Ag due to chloride ions. It has been shown that the catalyst support can play key role in preventing deactivation of catalyst during catalytic reactions (Agryle and Bartholomew, 2015; Yuan and Keane, 2003). The catalytic activity rapidly decreases as a result of loss of surface area, pore constriction, and ultimately pore blockage on the active sites (Jung et al., 2021).

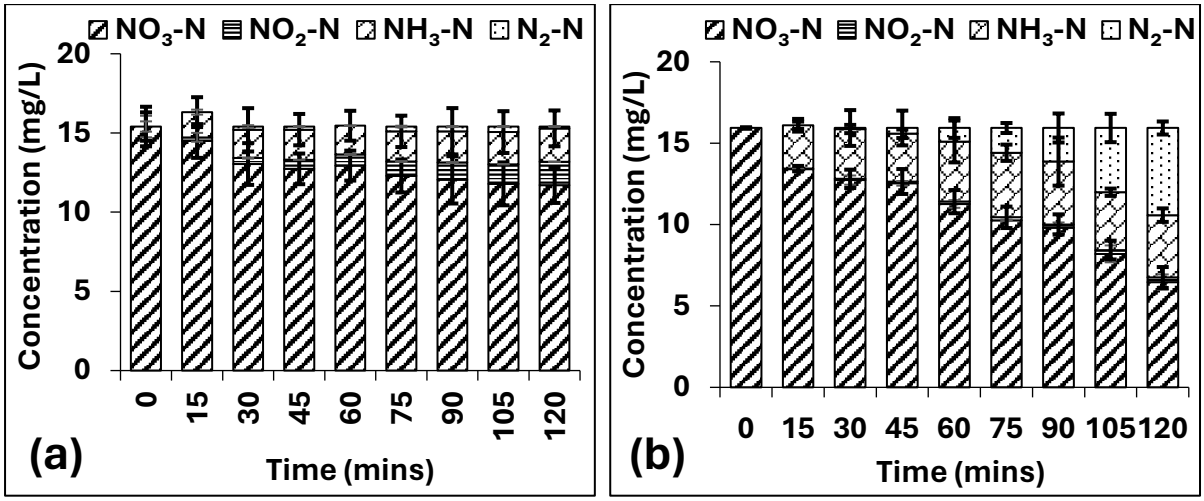

Figure 25 : Nitrate removal in the absence (a) and presence (b) of AgMPs in groundwater

(Reaction conditions: Groundwater, anode: Ti/RuO_2, cathode: Ti, 8mM Ag-PVA beads, Na_2SO_4: 2g/L as electrolyte, reaction time: 120 min)

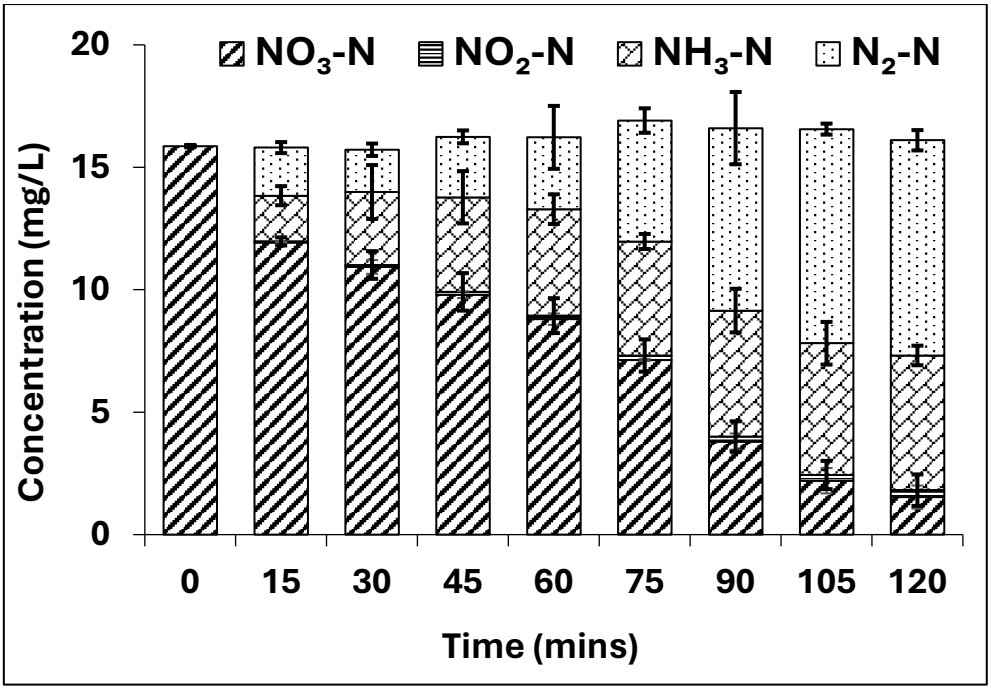

Figure 26 : Nitrate removal using Ti/Co_3O_4 in groundwater

(Reaction conditions: Groundwater, anode: Ti/RuO_2, cathode: Ti/Co_3O_4, Na_2SO_4: 2g/L as electrolyte, reaction time: 120 min)

Due to the reduced performance of suspended catalysts, it was pertinent to evaluate a catalyst which gives efficient removal of nitrate in real water as well as in the wastewater containing high nitrate concentration. Thus, we conducted ECR experiments using a Ti cathode with Co3O4 immobilized on it (Ti/Co_3O_4). Figure 34 shows the ECR of nitrate in groundwater using Ti/Co_3O_4 cathode and Ti/RuO_2 anode at 10mA/cm^2 current density for 120min electrolysis time. It is observed that using Ti/Co_3O_4 cathode, nitrate reduction increased with increasing selectivity towards nitrogen. 95% nitrate reduction was achieved resulting in 39 and 55% selectivity for NH_3-N and N_2-N, respectively.

Comparison of Figure 32, Figure 33, and Figure 34 shows that that the performance of Ti/Co_3O_4 for nitrate removal and selectivity for N_2-N was superior to the suspended silver catalysts. In the presence of Ag-PVA beads and AgMPs, nitrate reduction achieved was 85 and 59%, respectively whereas Ti/Co_3O_4 gave 95% nitrate reduction in real water (groundwater). Additionally, N_2-N selectivity in presence of Ag-PVA beads and AgMPs was 24 and 34%, respectively. N_2-N achieved in presence of Ti/Co_3O_4 was 55%. Less N_2-N selectivity was achieved using spatially suspended catalyst compared to Ti/Co_3O_4 and

this may be due to rapid deactivation of suspended catalyst (Ag-PVA beads and AgMPs) in the presence of chloride ions. The detrimental impact of Cl ions on inactivation of Ag catalyst was maximum compared to other anions (Sontakke et al., 2011). Experiments were also conducted under identical experimental conditions using spatially suspended catalyst (AgMPs) with immobilised catalyst (Ti/Co_3O_4). Figure 35 shows the ECR of nitrate using AgMPs with Ti/Co_3O_4 cathode. However, it may be noted that no significant improvement in nitrate removal was observed beyond that achieved in the absence of suspended catalysts.

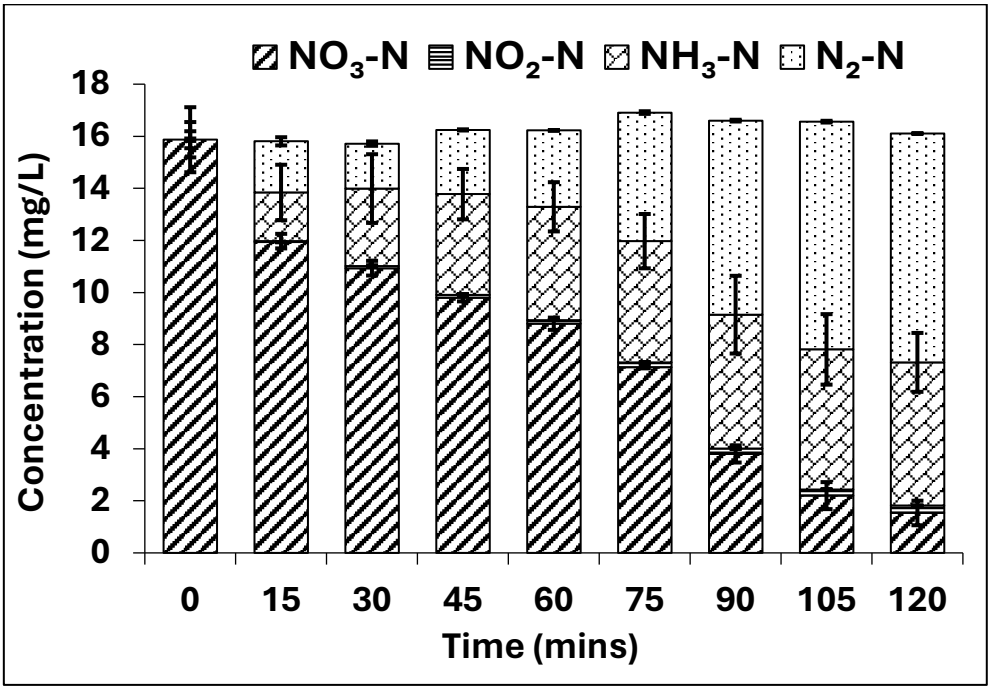

Figure 27 : Nitrate removal using AgMPs with Ti/Co_3O_4 in groundwater

(Reaction conditions: Groundwater, anode: Ti/RuO_2, cathode: Ti/Co_3O_4, 8mM AgMPs, Na_2SO_4: 2g/L as electrolyte, reaction time: 120 min)

For this reason, we explored the use of an immobilised catalyst (Ti/CO_3O_4) intending to increase the removal of nitrate and improve conversion to N_2-N while treating real water. So further, experiments for the ECR process were conducted using cathode-coated catalyst Ti/Co_3O_4 for high nitrate concentration in simulated metal finishing wastewater.

4.5 ECR of high nitrate concentration in metal finishing wastewater using catalyst-coated cathode (Ti/Co_3O_4)

This research study includes various parameters for ECR of high nitrate concentration from simulated metal finishing wastewater including initial nitrate-N concentration, current density, and reusability of Ti/Co_3O_4. Table 11 describes the characteristics of simulated metal finishing wastewater referred from Gabaldón et al. (2007).

Table 9: Characteristics of Simulated metal finishing wastewater

Parameters	Values
Nitrate-N	500-1000 mg/L
Sulphates	2000 mg/L
Chlorides	150 mg/L
Carbonates	75 mg/L
Bicarbonates	125 mg/L
pH	6.5-7.6
Zinc	15mg/L
Copper	15mg/L
Cadmium	10mg/L
Manganese	10mg/L
Nickel	10mg/L

4.5.1 XRD analysis of Ti/Co_3O_4

Figure 36 describes the XRD analysis of fresh and used Ti/Co_3O_4 electrodes. XRD is used to analyse the phase structures of Co_3O_4 films produced at the Ti plate. According to Figure 36, peaks suggest the cubic phase of the Co_3O_4 standard (JCPDS File No. #42-1467). Over time, pollutants including oxidation products, organic residues, or species present in wastewater may build up on the surface of a used plate. By interfering with the scattering of X-rays, these pollutants can alter the diffraction pattern and lessen the intensity of XRD peaks (Al-Nuaim et al., 2023; L. Yang et al., 2017). Thus, it can be depicted that a negligible difference is observed in the XRD analysis of fresh and used Ti/Co_3O_4.

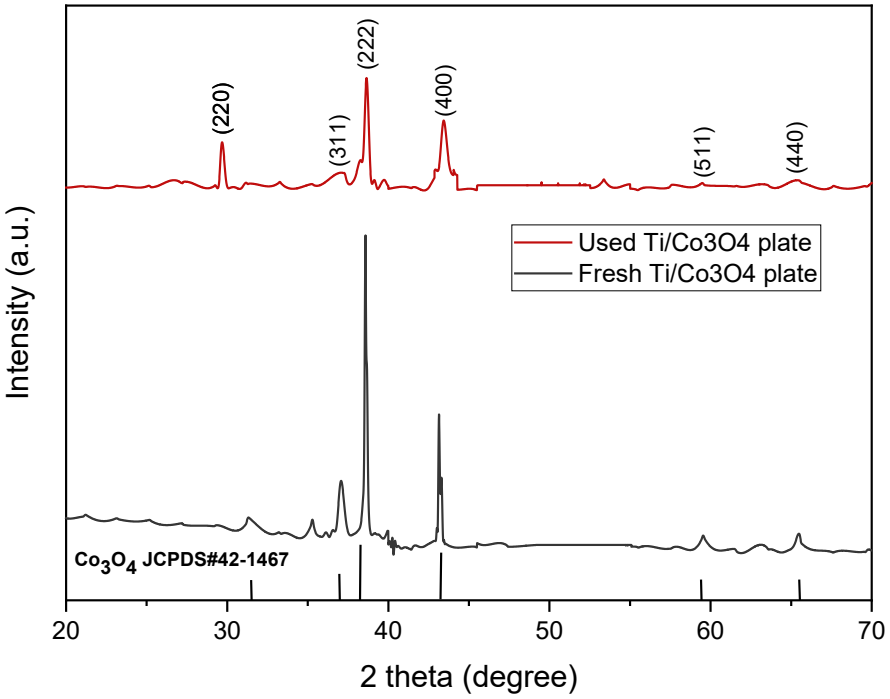

Figure 28 : XRD analysis of fresh and used Ti/Co_3O_4

4.5.2 Effect of the initial nitrate concentration

Figure 37 shows the effect of various initial nitrate-N concentrations (500, 750 and 1000 mg/L NO_3-N) on the reduction of nitrate at a current density of 20 mA/cm^2 using Ti/Co_3O_4 cathode and Ti/RuO_2 anode for 180 minutes of electrolysis time. Figure 33 demonstrates that nitrate removal was 97%, 95% and 90% for 500, 750, and 1000mg/L initial nitrate concentration, respectively. NO_2-N accumulation was <4 mg/L at the end of 180 min, irrespective of the initial nitrate-N concentration. However, accumulation of NH_3-N was ~95 mg/L at initial nitrate-N concentration of 500 mg/L and increased to ~190 mg/L at initial nitrate-N concentration of 1000 mg/L. Also, N_2-N generation marginally decreased as the initial nitrate concentration increased. Thus, the initial nitrate-N concentration did not have much impact on nitrate removal and product selectivity as products were formed according to the increasing rate of initial concentration.

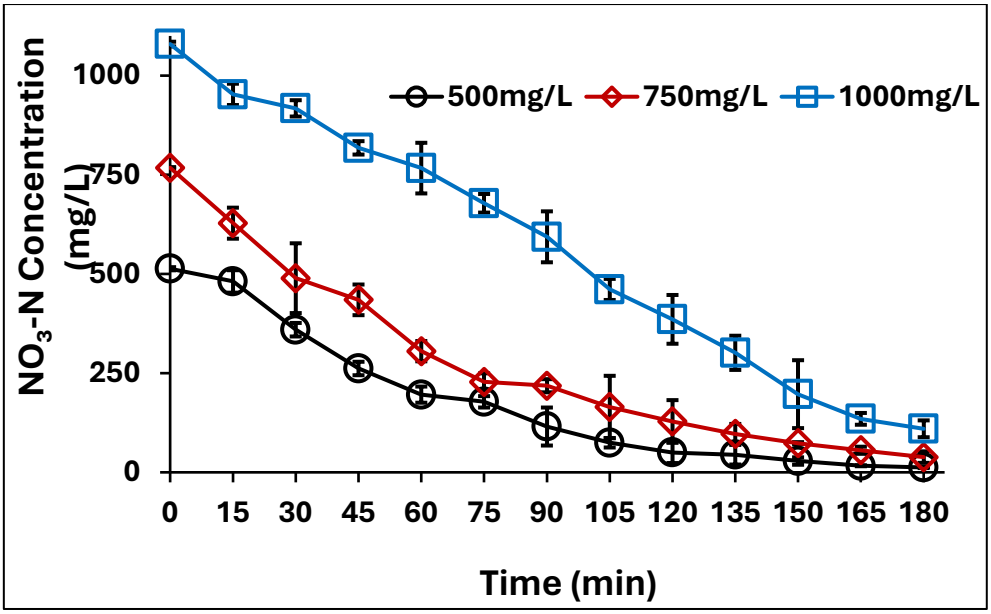
NO_3-N Concentration (mg/L)
1000
750
500
250
0
500mg/L
750mg/L
1000mg/L
0 15 30 45 60 75 90 105 120 135 150 165 180
Time (min)

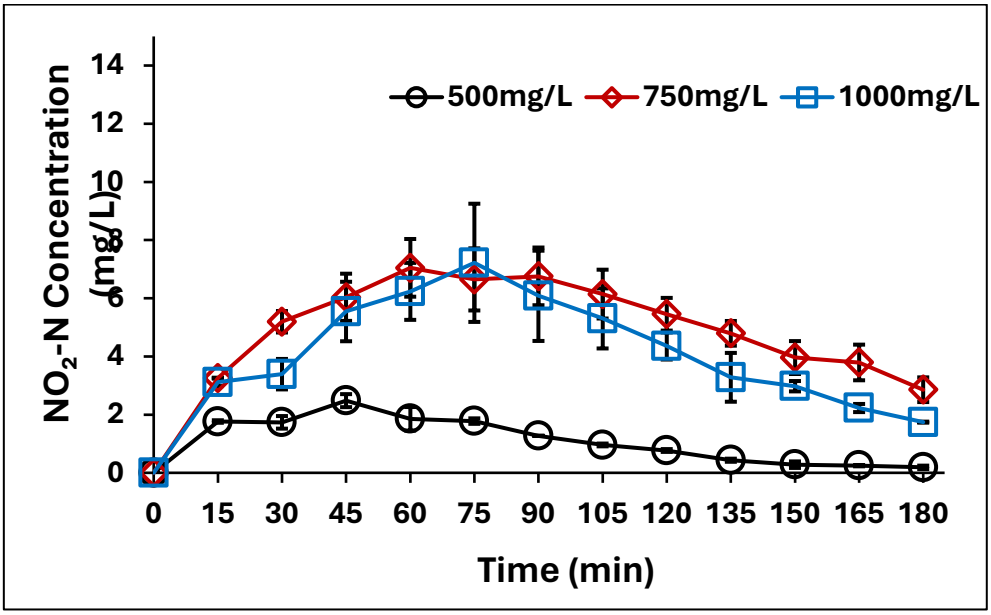
NO_2-N Concentration (mg/L)
14
12
10
8
6
4
2
0
500mg/L
750mg/L
1000mg/L
0 15 30 45 60 75 90 105 120 135 150 165 180
Time (min)

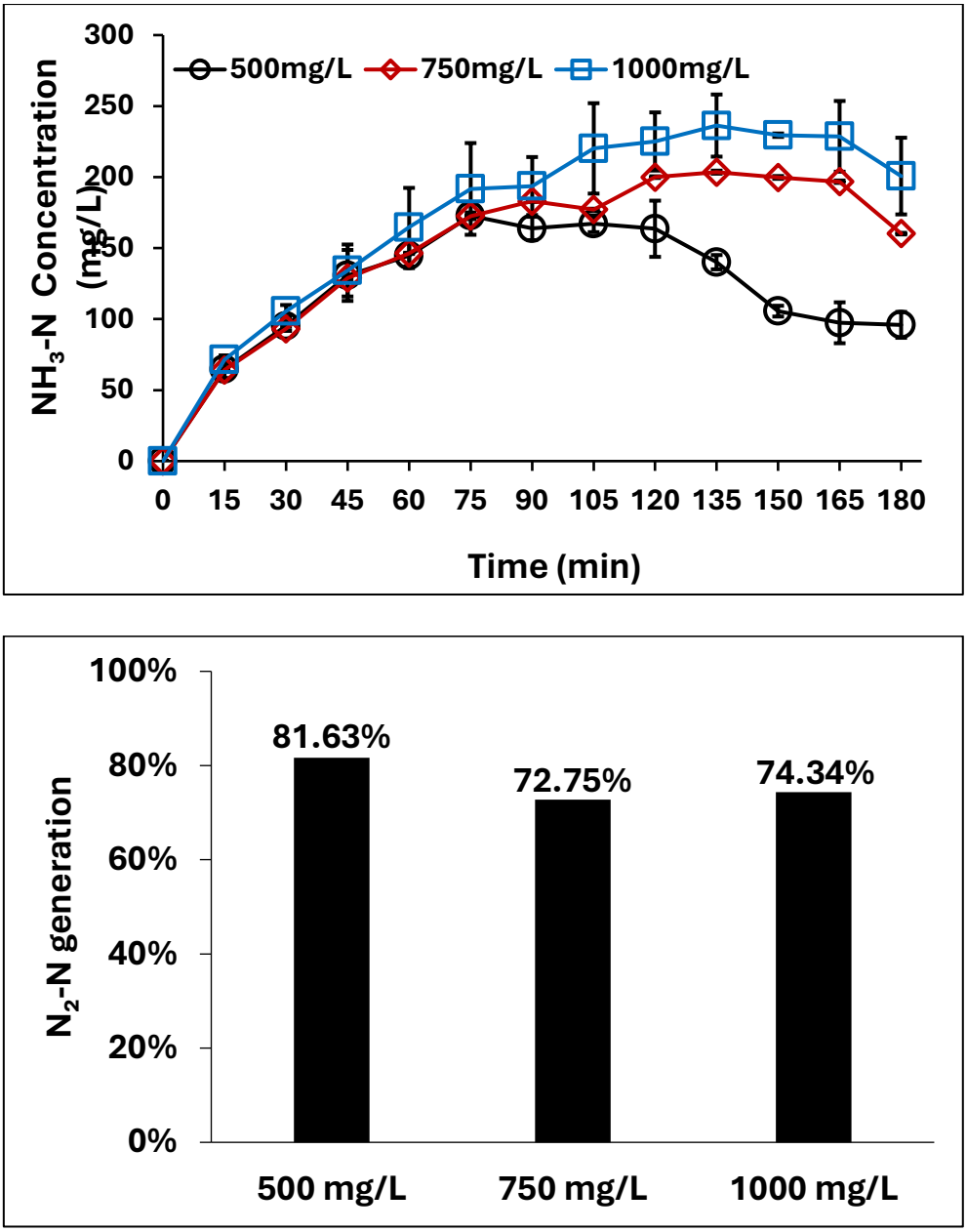

Figure 29 : Effect of initial nitrate concentration

(Reaction conditions: Cathode: Ti/Co_3O_4, Anode: Ti/RuO_2, current density: 20mA/cm^2, Na2SO4 electrolyte: 2g/L, reaction time: 180min)

Su et al. (2017) studied nitrate removal by ECR process in actual textile wastewater and they observed that after 3 hours of treatment at 25 mA/cm^2 current density, the NO_3-N removal efficiency for raw wastewater was 59%. A little amount of NH_4-N (1%) was found, and 58% of the TN was successfully removed. Also, authors studied NO_3-N removal efficiency of Fenton pretreated wastewater using Ti/Co_3O_4 cathode. They achieved 93%

nitrate removal with 32% NH_4-N generation. NO_2-N was negligible and TN removal was 61% after 3hrs of treatment.

4.5.3 Effect of current density

Current density is one of the factors that has the most impact on the electrochemical reduction process. . Studies were conducted using Ti/Co_3O_4 cathode and Ti/RuO_2 anode for 180min electrolysis time to determine the effect on the selectivity for the end-products and nitrate removal at current densities of 10, 20 and 30 mA/cm^2. Figure 38 shows that at current densities of 10, 20 and 30 mA/cm^2, respectively, NO_3-N removal was 74, 95, and 100%, whereas TN removal was 45%, 74%, and 79%. N_2-N selectivity increased as the current density increased. It was observed that N_2-N selectivity was almost similar with 20 mA/cm^2 and 30 mA/cm^2 current density.

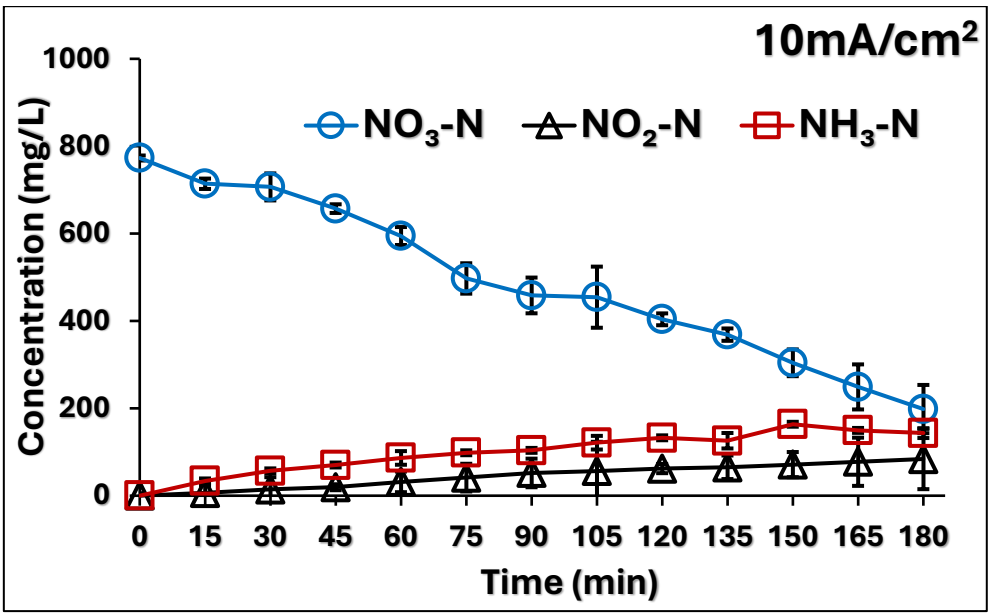

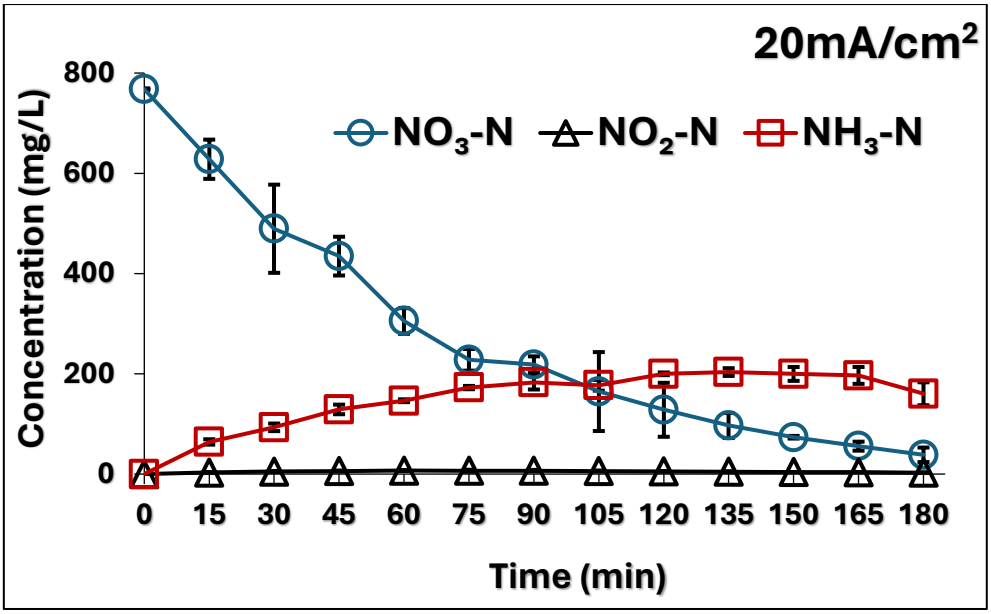
20mA/cm2
Concentration (mg/L)
800
600
400
200
0
NO3-N
NO2-N
NH3-N
0 15 30 45 60 75 90 105 120 135 150 165 180
Time (min)

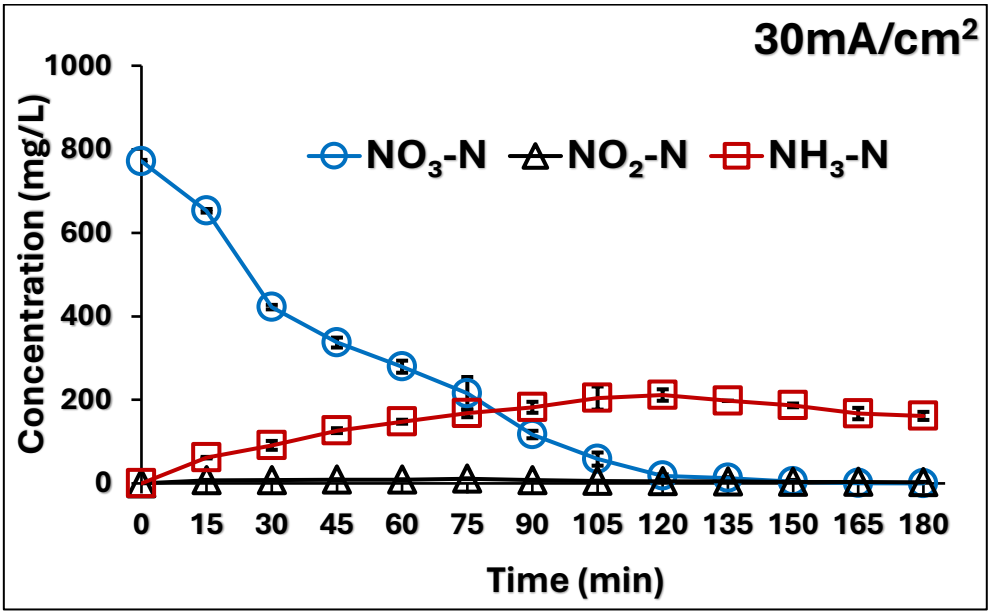
30mA/cm2
Concentration (mg/L)
1000
800
600
400
200
0
NO3-N
NO2-N
NH3-N
0 15 30 45 60 75 90 105 120 135 150 165 180
Time (min)

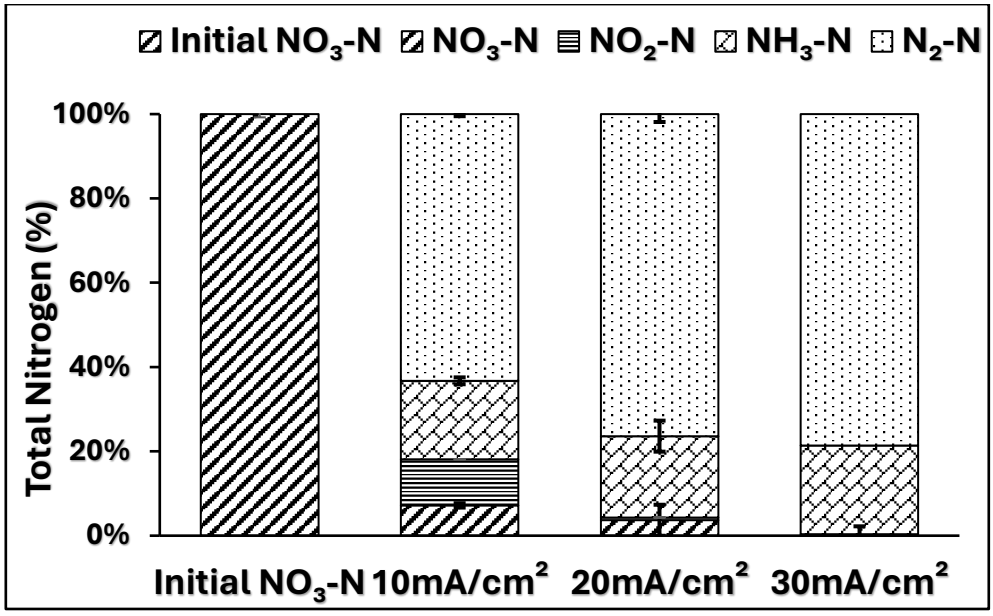

Figure 30 : Effect of current density on nitrate removal

(Reaction Conditions: Simulated metal finishing wastewater NO_3-N Concentration: 750 mg/L, cathode: Ti/Co_3O_4, anode: Ti/RuO_2, reaction time: 180 min; inter-electrode distance: 7.7cm)

W. Li et al. (2016) examined the nitrate removal in a divided cell at various current densities. The nitrate removal efficiency rose steadily as the current density rose from 5 to 20 mA/cm^2. However, from 15 mA/cm^2 to 20 mA/cm^2, the nitrate removal rate increased slowly. So, the optimum nitrogen selection rate was found at a current density of 15 mA/cm^2. Sahu et al. (2014) stated that increasing current density boosts nitrate removal performance, however, excessive current density also promotes electrode corrosion and dissolution. Also, it increases the energy consumption of the electrocatalytic system.

Thus, N_2-N was the major product obtained at the end of the treatment. Further, we conducted experiments to study the lifespan of Ti/Co_3O_4 electrodes.

4.5.4 Reusability of Ti/Co_3O_4

Catalysts must have a longer life span in order to be used on a wider scale. Figure 39 illustrates the ability of Ti/Co_3O_4 electrodes to be recycled for NO_3-N reduction. Experiments were conducted at 20mA/cm^2 using Ti/Co_3O_4 cathode and Ti/RuO_2 anode for 750mg/L NO_3-N concentration in simulated metal finishing wastewater for 60min of reaction time. As can be seen, the Ti/Co_3O_4 electrode can be used for 12 continuous

reaction cycles before showing any detectable loss in catalytic activity. It is noteworthy to observe that ammonia formation changed after the 12th cycle to become more selective. Sloughing of the cobalt oxide layer was noticed after 15 number of cycles. ICP (Inductively Coupled Plasma) was used to determine the concentration of dissolved cobalt in the treated solution, and it was found that only 0.06mg/L was present after 180min of reaction time. ICP was also used to detect the concentration of metals in treated wastewater is shown in Figure 40. All metals present in simulated metal finishing wastewater were efficiently removed during the ECR process. It is possible that some of the metal ions may be reduced in the cathode compartment and deposited on Ti/Co_3O_4 cathode altering the selectivity of end-products after repeated uses.

Y. Zhang et al. (2018) investigated reusability of Cu/Ni (copper on nickel foam) electrode for nitrate reduction in real textile wastewater and reported that Cu/Ni electrode can be used for 8cycles without leaching Cu during the treatment.

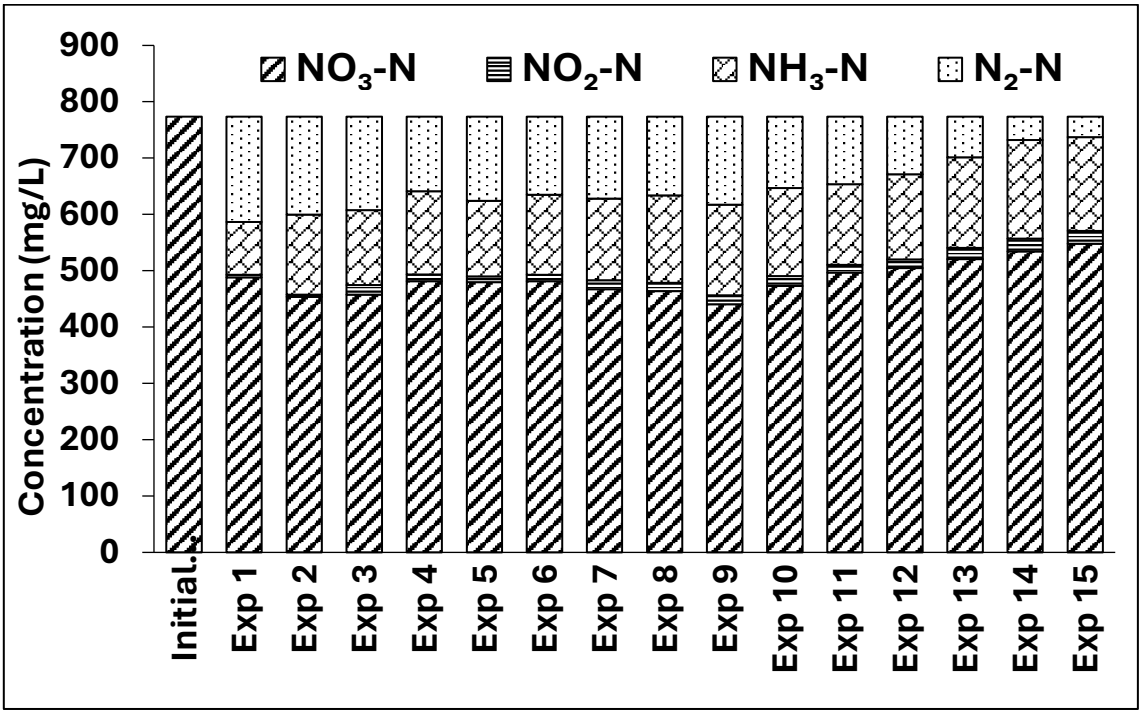

Figure 31 : Reusability of Ti/Co_3O_4 cathode

(Reaction Conditions: Anode: Ti/RuO_2; cathode: Ti/Co3O4; current density: 20mA/cm^2; simulated metal finishing wastewater containing nitrate-N: 750mg/L; reaction time 60min)

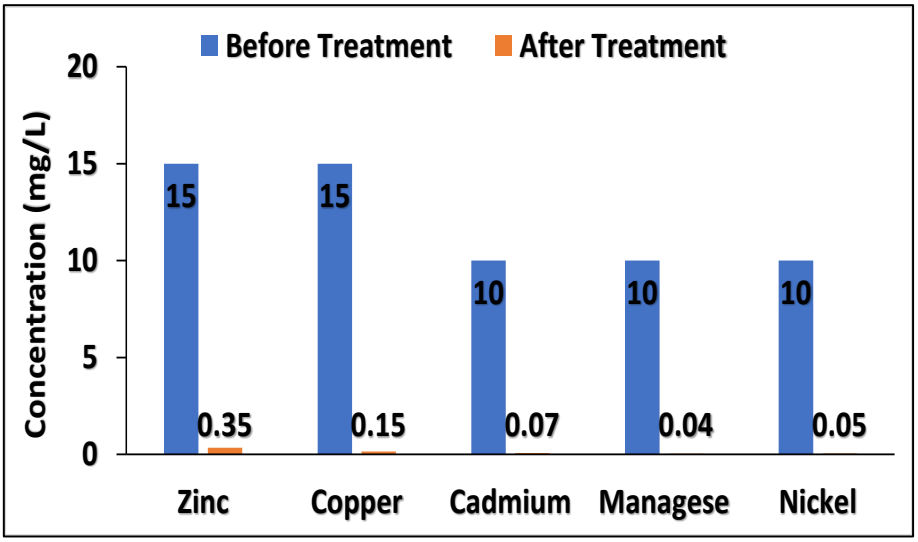

Figure 32 : Concentration of metals before and after treatment

(Reaction Conditions: Anode: Ti/RuO_2; cathode: Ti/Co_3O_4; current density: 20mA/cm^2; simulated metal finishing wastewater containing nitrate-N: 750mg/L; reaction time 180min)

During the ECR process for nitrate-N removal in simulated metal finishing wastewater, white precipitated were formed. Besides the reduction of metal ions to corresponding metal form, the metal ions may also get precipitated as metal hydroxide due to high pH in the cathode compartment. These precipitates were collected as they were easily settleable and dried at room temperature for XRD analysis. Metal hydroxides might develop in the cathode compartment during the reaction due to the alkaline pH (≈12) conditions. Figure 41 shows the XRD analysis of precipitates and its comparison with JCPDS standard files of metal hydroxides present in the precipitates. It can be seen that the XRD peaks of precipitates are identical with the XRD peaks of metal hydroxides contain present in the treated metal finishing wastewater.

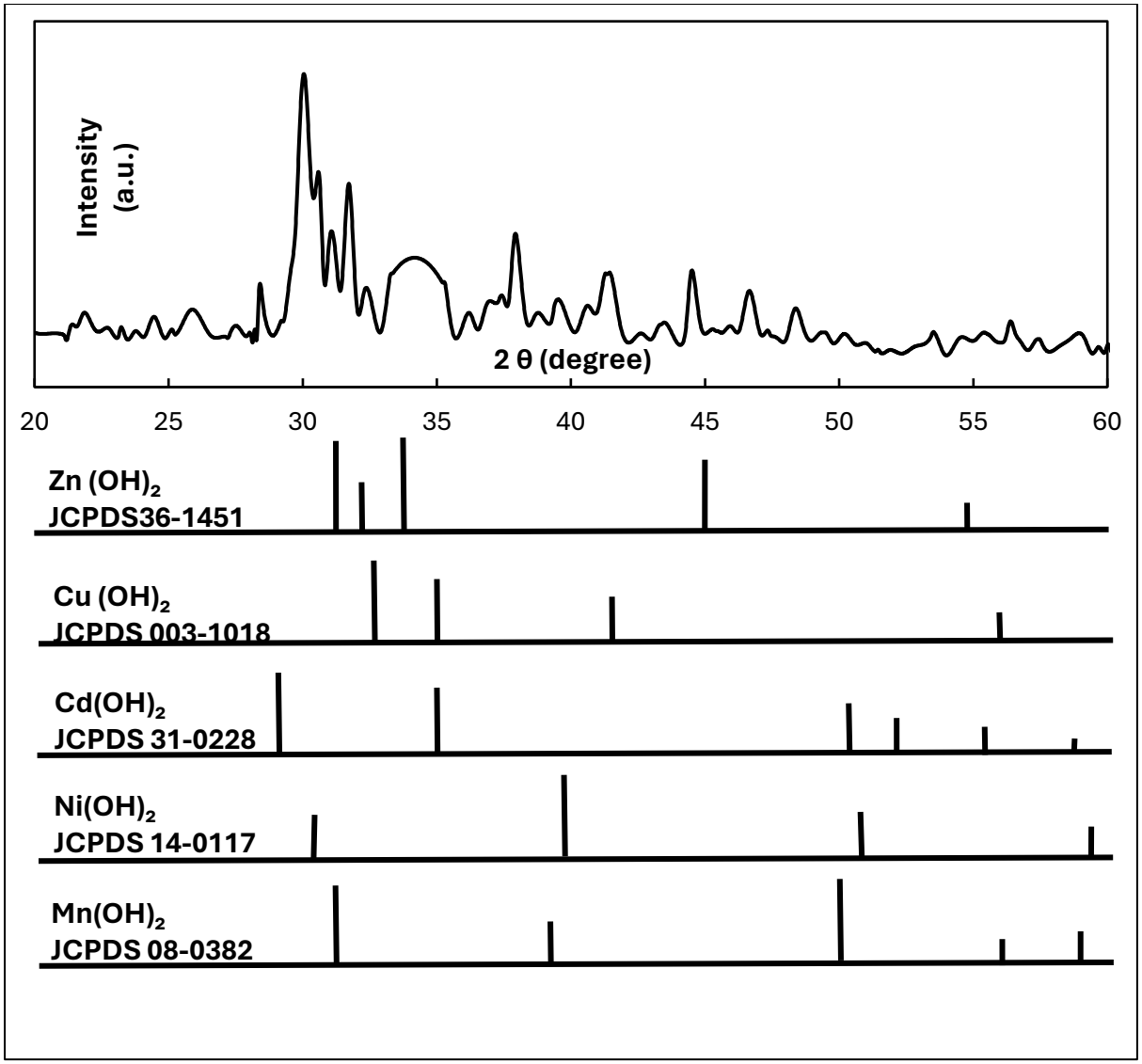

Figure 33 : XRD analysis of precipitates formed in treated water

4.5.5 Struvite formation for ammonia removal

As noted in section 4.5.2, during the ECR of metal finishing wastewater, the accumulation of NH_3-N was as high as ~190 mg/L at the initial nitrate concentration of 1000 mg/L. The discharge limit for NH_3-N in the treated wastewater is 50 mg/L in India. Thus, it was necessary to remove ammonia. Precipitation of ammonia as struvite is an efficient method to recover ammonia for use as a fertilizer. Struvite (magnesium ammonium phosphate) is a substance that is frequently used in wastewater treatment operations to remove ammonia. Struvite crystals develop when there is enough amount of magnesium, ammonium, and phosphate ions, and they either adsorb or integrate the ammonium ions (Perera et al., 2019). As a result, the ammonia in the effluent is

eliminated. It provides a considerate method for reducing ammonia levels and recovering valuable substances from wastewater.

Struvite offers several benefits: (1) Struvite precipitation can efficiently remove ammonia from wastewater and lower the content to tolerable limits (Kumar & Pal, 2015). (2) Resource recovery: because struvite includes phosphate and nitrogen, which can be extracted and used to make fertilisers or other useful products (Puchongkawarin et al., 2015; Ryu et al., 2012; Talboys et al., 2016). (3) Ammonia may corrode and foul pipelines, pumps, and other equipment. Struvite removal increases the lifespan of the wastewater treatment system and protects the infrastructure. In general, a pH of around 9 (González-Morales et al., 2021; Hao et al., 2008) is considered optimal for struvite formation, as it provides the necessary conditions for the precipitation of magnesium, ammonium, and phosphate ions to form struvite crystals.

Our study includes the removal of remaining ammonia generated from the ECR of nitrate by struvite formation. XRD analysis was carried out to study the crystallography of struvite. Additionally, the effect of various molar ratios of $Mg:NH_4:PO_4$ (0.8:1:0.8, 1:1:1, 1.5:1:1; 1:1:1.5 and 1.5:1:1.5) on struvite formation were studied by adjusting pH at 9. For phosphate analysis, a colorimetric method (stannous chloride method, APHA Methods 4-163) was used.

XRD analysis of struvite ($Mg:NH_4:PO_4$ = 1.5:1:1.5) is shown in Figure 42. For struvite analysis, the sample was dried at room temperature for 24hrs, and the dried sample was used for XRD analysis. Peaks were discovered at various angles which correspond to the Braggs reflections of the facets of the crystal planes at 2θ which was confirmed by JCPDS File No. 77-2302 for struvite. The XRD peaks observed in the struvite formed in the present study also closely matched with those reported by Lee et al. (2015) and Jabr et al. (2019).

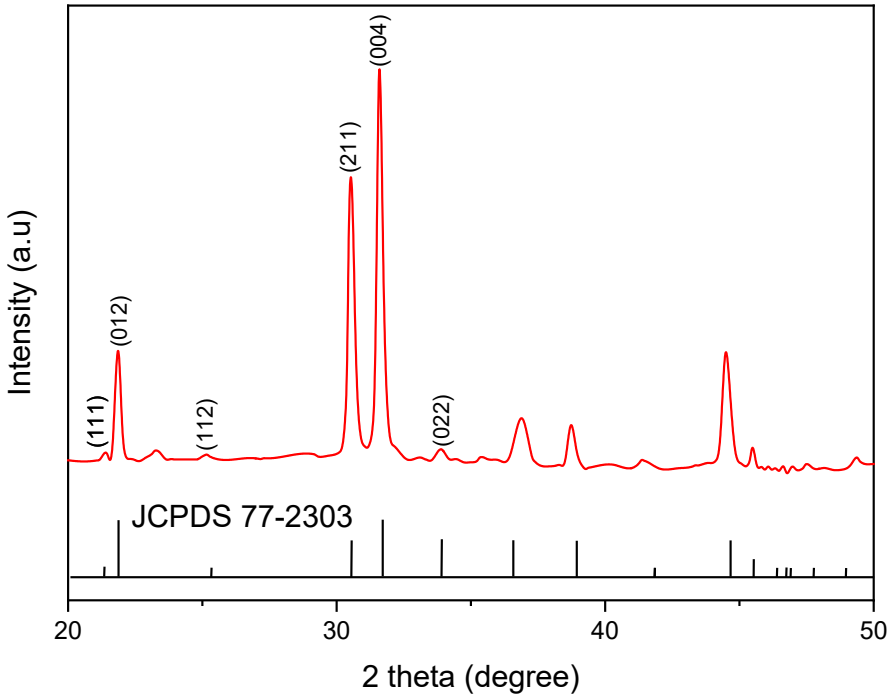

Figure 34 : XRD analysis of struvite

4.5.5.1 Effect of molar ratios of Mg:NH_4:PO_4 on struvite formation for removal of ammonia

Figure 43 shows various struvite molar ratios of Mg:NH_4:PO_4 (0.8:1:0.8, 1:1:1, 1.5:1:1, 1:1:1.5 and 1.5:1:1.5) at pH 9 on struvite formation were studied to remove remaining ammonia from treated metal finishing wastewater. A 1.5:1:1.5 molar ratio was found to be the most effective for removing the most ammonia, which allowed concentrations of wastewater from simulated metal finishing processes with high nitrate content to be finally processed while removing ammonia below discharging levels. 80% ammonia was removed by struvite formation with minimum residual of PO_4 (3.5-3.8mM).

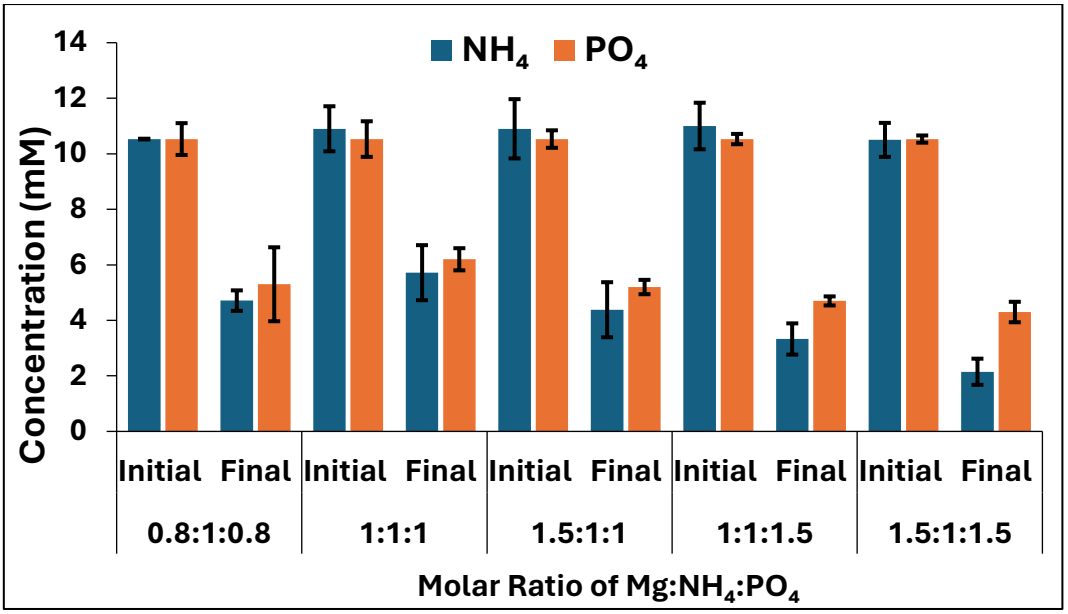

Figure 35 : Ammonia removal by struvite formation

Zhou & Wu, (2012) showed that 98% ammonia-N was removed with 2.32mg/L PO_4^{3}-P residue at 1.10:1:1.31 molar ratio of Mg/N/P. One factor that contributed to the molar ratio exceeding the predicted value of Mg/N/P 1:1:1 was the synthesis of $Mg_3(PO_4)_2$, which slowed the pace of struvite precipitation and resulted in the usage of Mg_2^+ in unpredictably high levels (Ohlinger et al., 1998). This meant that driving out all available phosphate that was accessible could need a surplus of magnesium. In fact, the majority of the reported molar ratios in the literature were frequently at odds with the ones predicted by theory. According to the literature, the observed Mg/N and P/N values ranged from 1.1 to 1.67 are suitable (Parsons & Doyle, 2002).